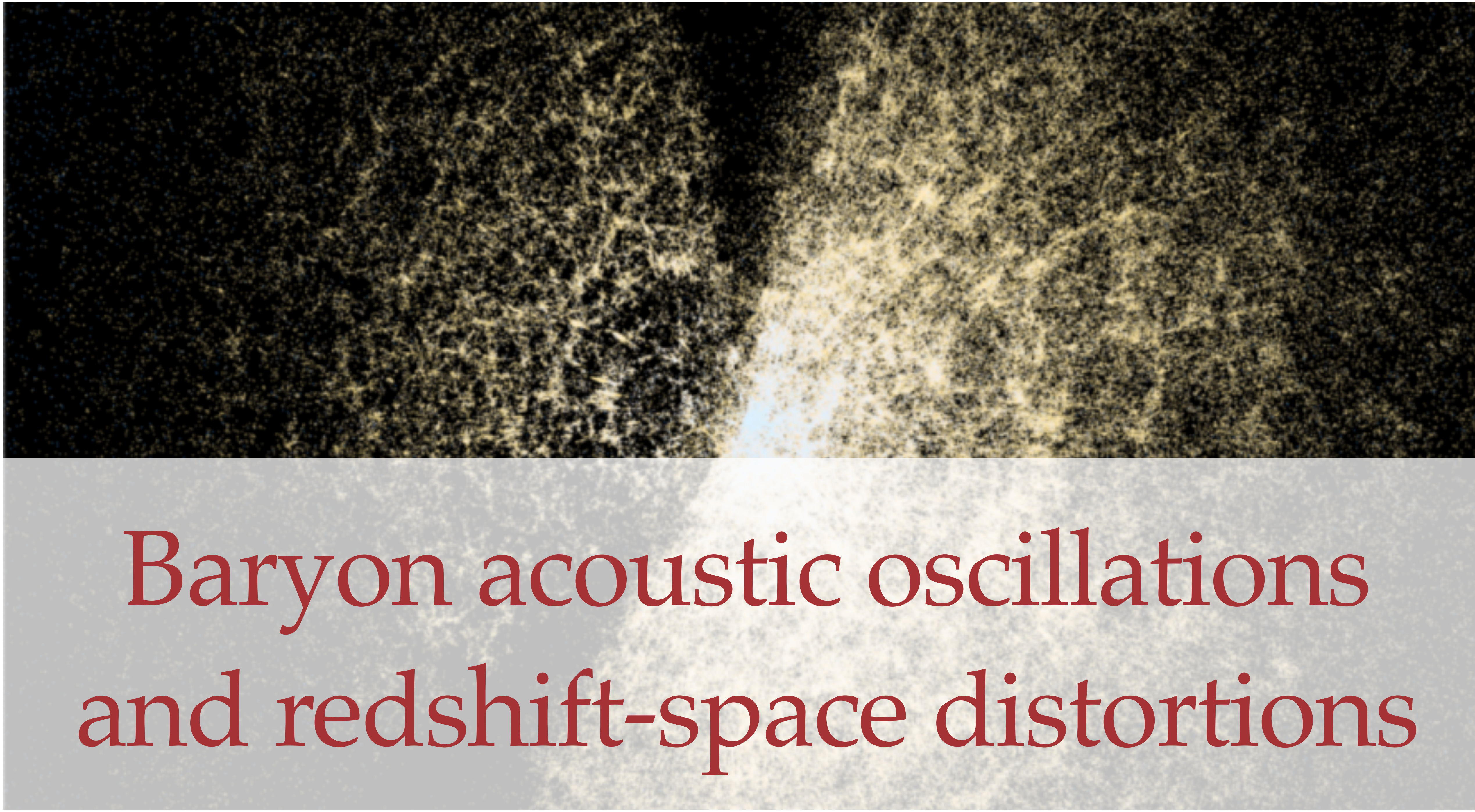

Baryon acoustic oscillations and redshift-space distortions

Ariel G. Sánchez

MAX-PLANCK-GESELLSCHAFT

LAPIS 2018: Cosmology in the era of large surveys - 23.04.2018

Lecture 1: BAO

- Introduction: cosmology from LSS observations.
- Baryon acoustic oscillations (BAO).
- Galaxy redshift surveys.
- Potential systematic errors.
- Angle-averaged vs anisotropic measurements.
- Present-day BAO measurements.

Lecture 2: RSD

- Redshift-space distortions (RSD).
- The density - velocity relation.
- Impact of RSD on clustering measurements.
- Modelling of RSD beyond the linear regime.
- Current cosmological constraints from BAO & RSD.
- Forecasts for future surveys.

Redshift-space distortions

- The LSS of the Universe as traced by galaxies.

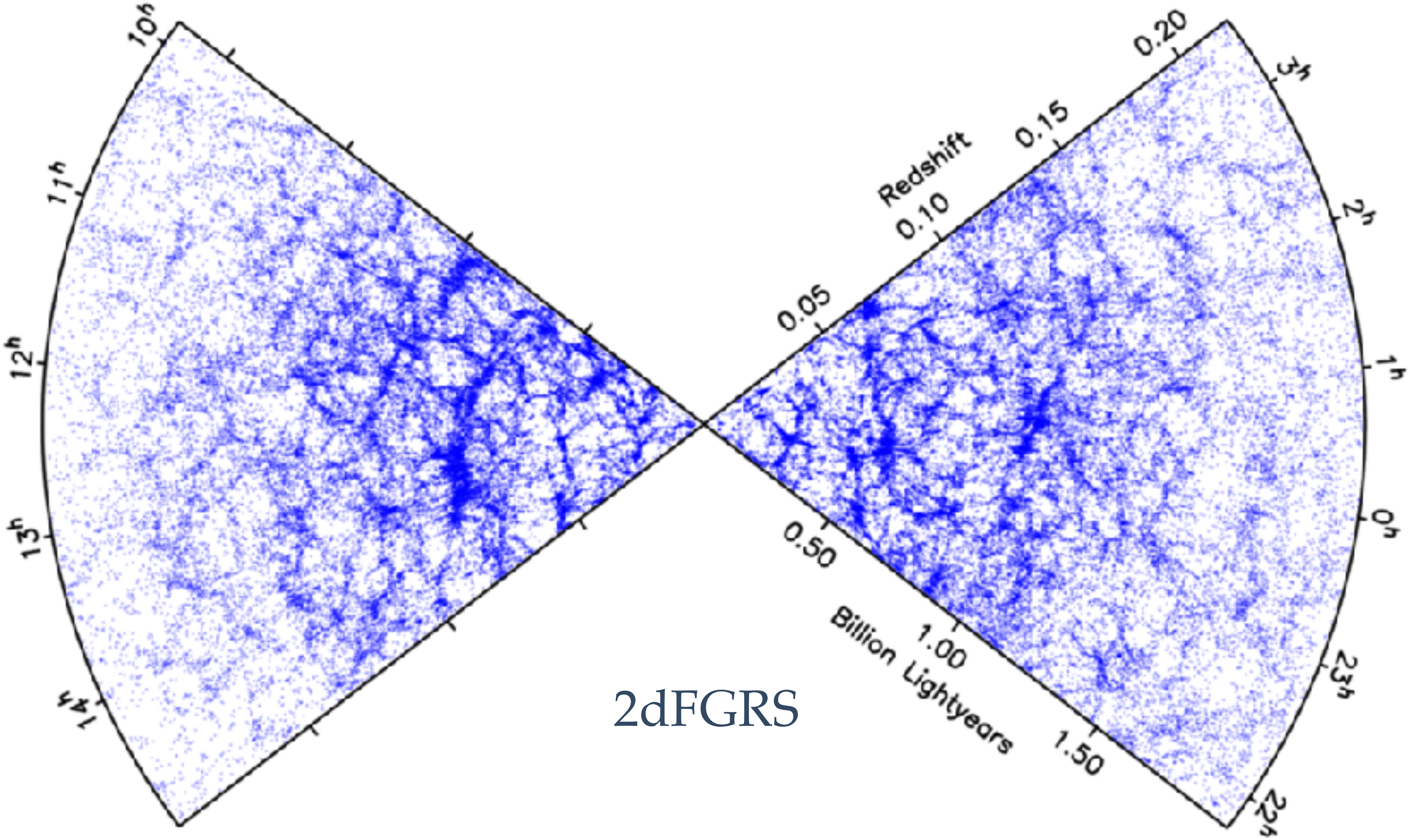

2dFGRS

Redshift-space distortions

- The observed redshifts are affected by peculiar velocities.

$$(1 + z_{\rm obs}) = (1 + z_{\rm cos})(1 + v/c)$$

- Velocities depend on the density field itself.

- RSD are a probe of the density-velocity relation.

- Constrain the growth-rate of cosmic structure.

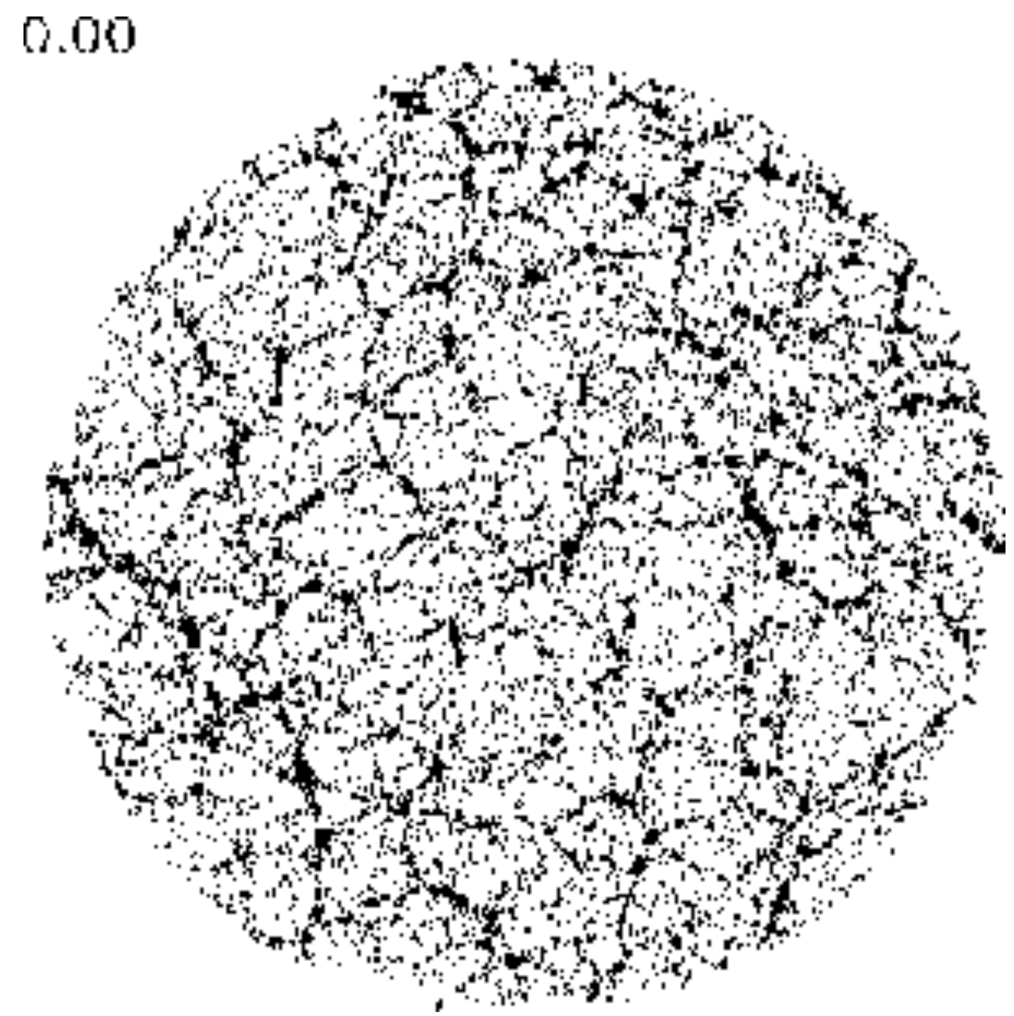

Figure: Hume Feldman

Redshift-space distortions

- The observed redshifts are affected by peculiar velocities.

$$(1 + z_{\text{obs}}) = (1 + z_{\text{cos}})(1 + v/c)$$

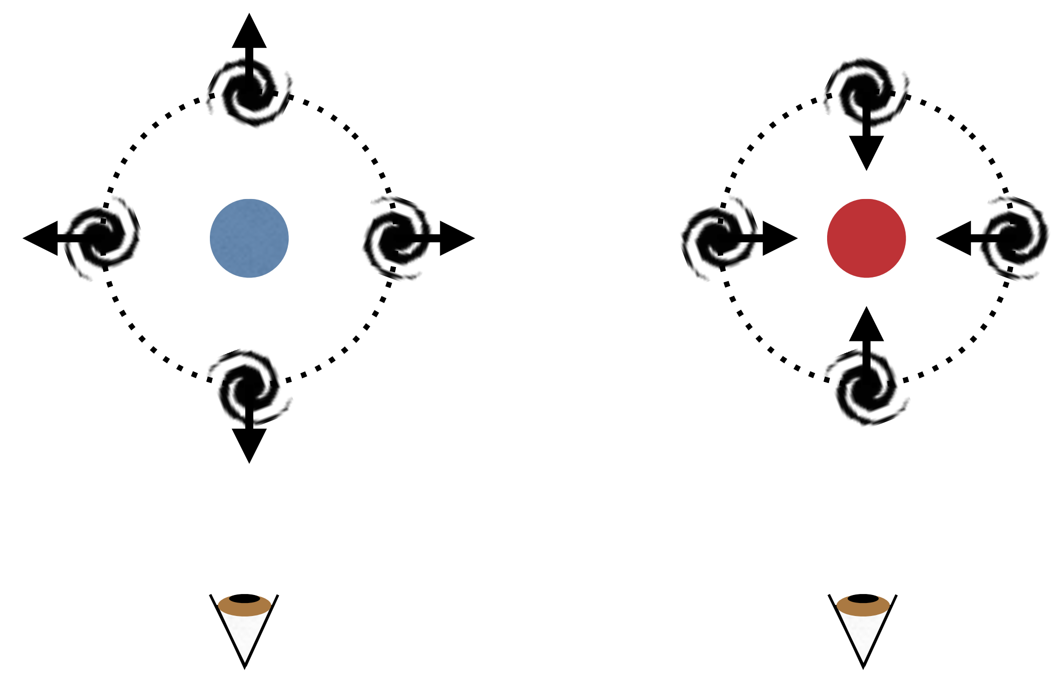

- Velocities depend on the density field itself.
- RSD are a probe of the density-velocity relation.
- Constrain the growth-rate of cosmic structure.

Redshift-space distortions

- The observed redshifts are affected by peculiar velocities.

$$(1 + z_{\mathrm{obs}}) = (1 + z_{\mathrm{cos}})(1 + v/c)$$

- Velocities depend on the density field itself.

- RSD are a probe of the density-velocity relation.

- Constrain the growth-rate of cosmic structure.

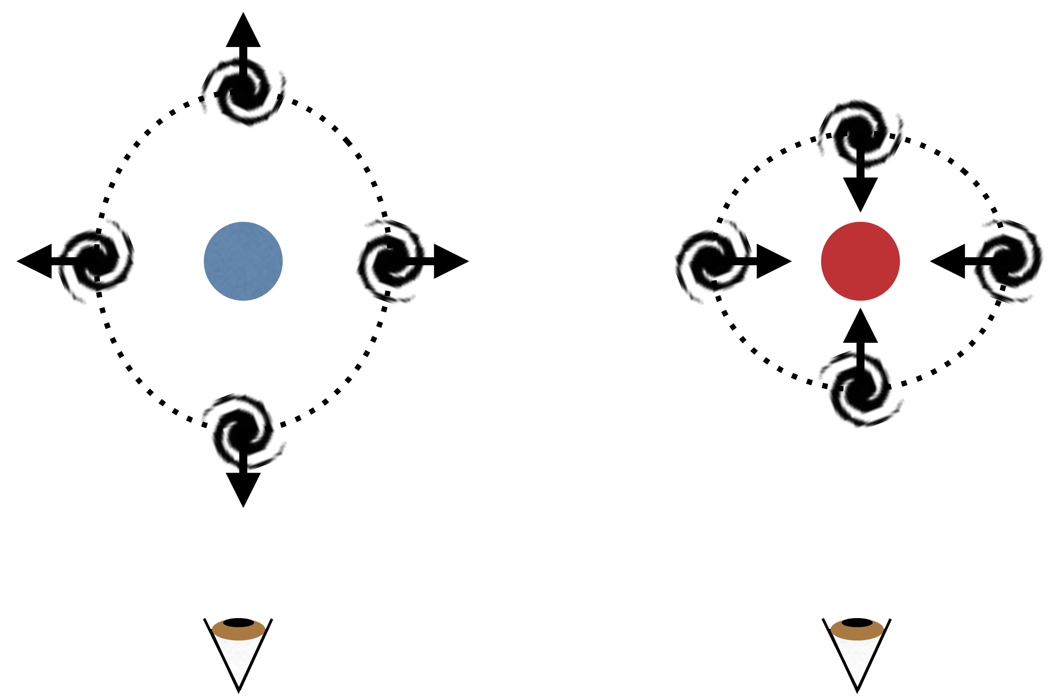

Redshift-space distortions

- The observed redshifts are affected by peculiar velocities.

$$(1 + z_{\rm obs}) = (1 + z_{\rm cos})(1 + v/c)$$

- Velocities depend on the density field itself.

- RSD are a probe of the density-velocity relation.

- Constrain the growth-rate of cosmic structure.

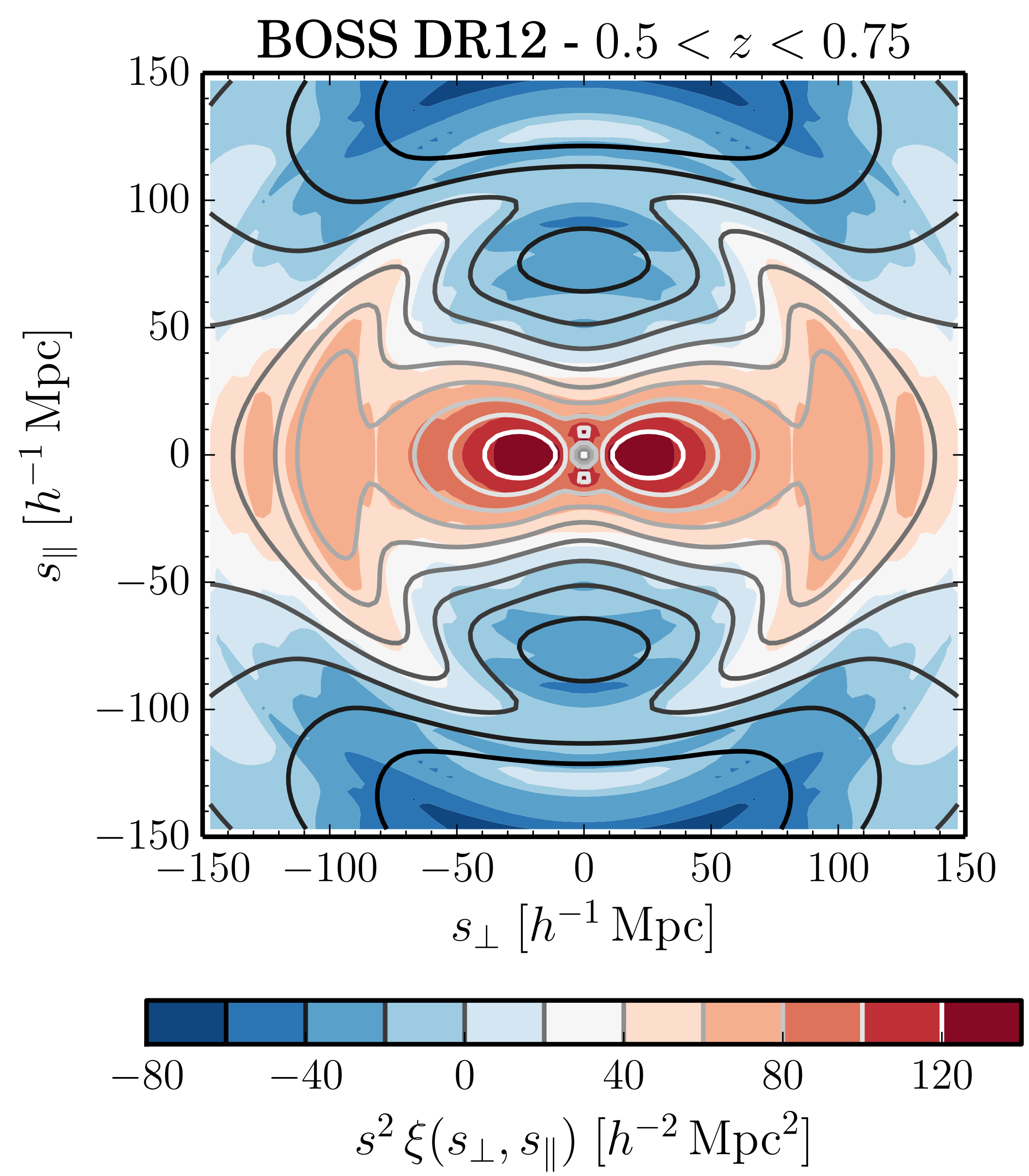

$$f(z) = \frac{\mathrm{d}\ln D}{\mathrm{d}\ln a}$$

The growth of density fluctuations

- The evolution of $\delta_{\rm m}$ follows the continuity, Euler and Poisson equations.

- Sub-horizon modes ($k \gg \mathcal{H}$) are described by

$$\delta_{\rm m}'' + 2\mathcal{H}\delta_{\rm m}' - 4\pi G a^2 \rho \delta_{\rm m} = 0$$

- The solution to this equation is known as the *growth factor*

$$D_1 = \frac{5\Omega_{\rm m}}{2}\frac{H(a)}{H_0}\int_0^a \frac{da_1}{(a_1 H(a_1)/H_0)^3}$$

- Normalised to give $D_1 = a$ during matter domination.

The peculiar velocity field

- The evolution of $v_{\rm m}$ is given by the continuity equation.

$$\delta_{\rm m}' - k^2 v_{\rm m} = 0$$

Using the fact that $\Phi' = 0$ during matter dom.

- Using our solution for $\delta_{\rm m}$ we find

$$v = \frac{1}{k^2}\left[\frac{\delta_{\rm m}(k,\tau)}{D_1} D_1\right]' = \frac{\delta_{\rm m}(k,\tau)}{k^2 D_1(\tau)} D_1'.$$

- Using that $d/d\tau = a\mathcal{H} d/da$ and defining

$$f \equiv \frac{a}{D_1}\frac{dD_1}{da} = \frac{d\ln D_1}{d\ln a} \quad \longrightarrow \quad v(k,a) = \frac{\mathcal{H} f(a)}{k^2}\delta_{\rm m}(k,a).$$

The peculiar velocity field

- The velocity field is given by the gradient of $v_{\rm m}$

$$v_j(k,a) = i\frac{k_j}{k^2}\mathcal{H}f(a)\delta_{\rm m}(k,a)$$

- The growing mode of the velocity field represents matter flowing to/from over/under-dense regions.

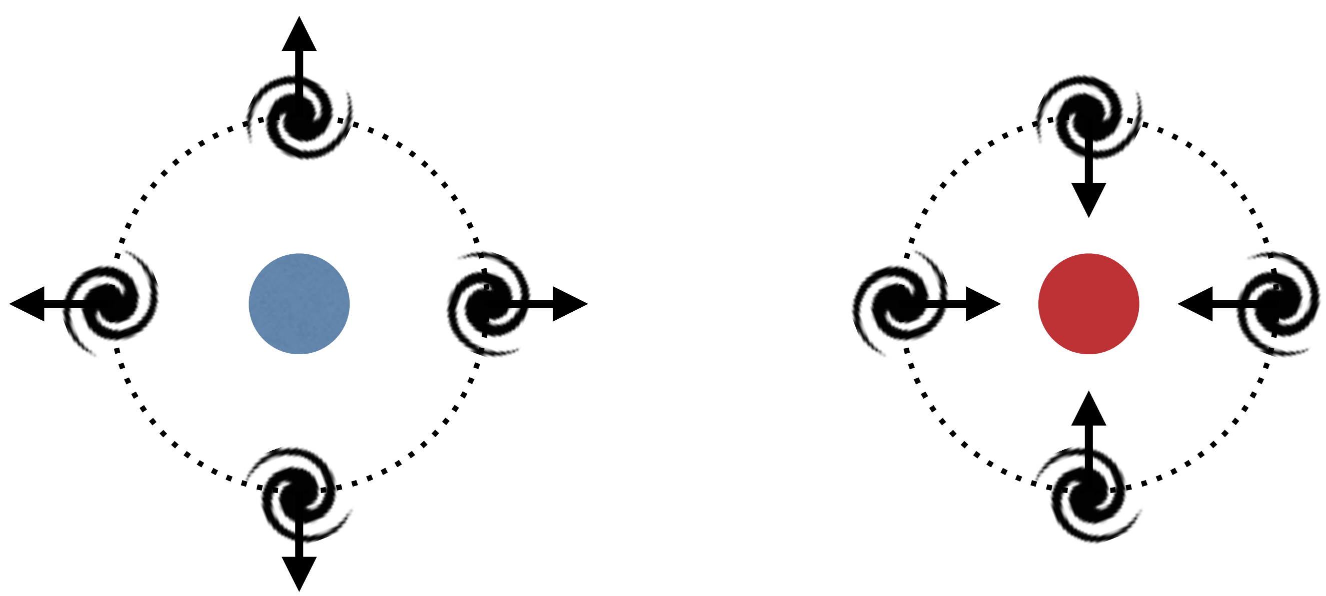

The peculiar velocity field

- The velocity field is given by the gradient of v_{m}

$$v_j(k,a) = i\frac{k_j}{k^2}\mathcal{H}f(a)\delta_{\mathrm{m}}(k,a)$$

- The growing mode of the velocity field represents matter flowing to/from over/under-dense regions.

- Measurements of $\mathbf{v}_{\mathrm{m}}$ and δ_{m} allow us to measure $f(a)$.

- Possible test of deviations from the predictions of GR.

$$f(z) \cong \Omega_m(z)^{0.55}$$

GR prediction that can be tested.

The impact of peculiar velocities

- The observed redshifts are given by

$$z_{\rm obs} = z + (1+z)\frac{v_\parallel}{c}$$

- Using $z_{\rm obs}$ to infer the distance to a galaxy we find

$$\begin{aligned} s = \chi(z_{\rm obs}) &= \chi(z) + \frac{d\chi}{dz}(z)\Delta z, \\ &= \chi(z) + \frac{1}{\mathcal{H}(z)} v_\parallel . \end{aligned}$$

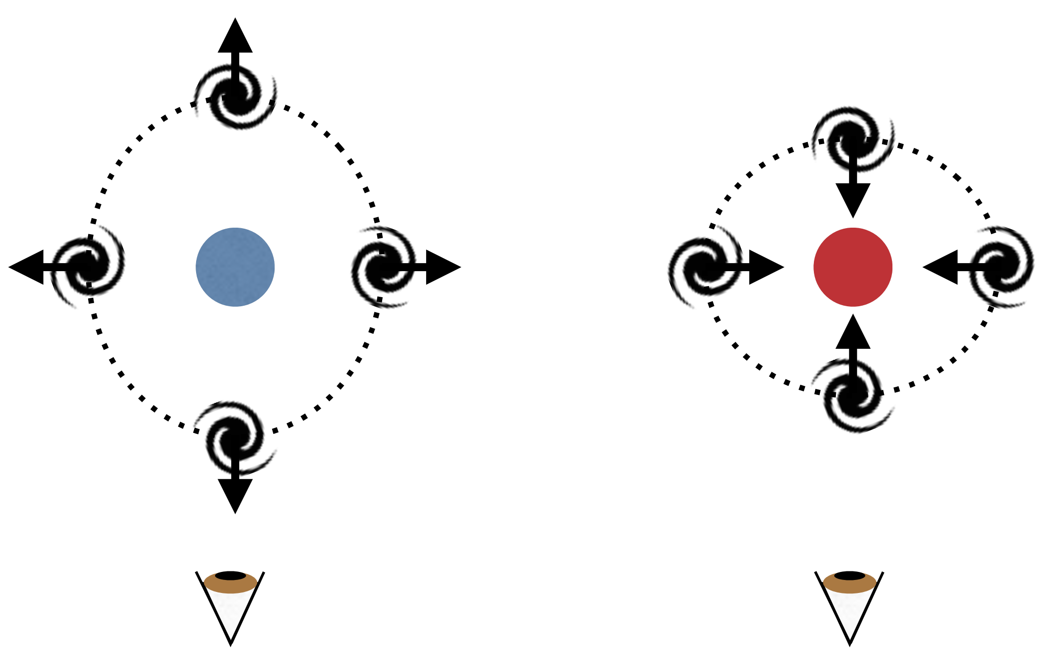

Redshift-space distortions

- RSD do not change the total number of galaxies

$$n(\mathbf{s})\,\mathrm{d}^3 s = n(\mathrm{r})\,\mathrm{d}^3 r$$

$$(1+\delta^{\mathrm{s}}(\mathbf{s}))\ d^3 s = (1+\delta(\mathbf{r}))\ d^3 r$$

- The volume elements are related by the Jacobian

$$J = \left(1 + \frac{1}{\mathcal{H}(z)}\frac{\partial v_3}{\partial r_3}\right)^{-1} \simeq \left(1 - \frac{1}{\mathcal{H}(z)}\frac{\partial v_3}{\partial r_3}\right)$$

- Using the solution for the peculiar velocity field, we find

$$\delta^{\mathrm{s}}(\mathbf{k}) = \delta(\mathbf{k})\left(1 + f(z)\mu_k^2\right) \qquad \mu_k = k_3/k$$

- The power spectrum is then given by (Kaiser 1987).

$$P^{\mathrm{s}}(k,\mu_k) = \left\langle |\delta^{\mathrm{s}}(k,\mu_k)|^2 \right\rangle = \left(1 + f(z)\mu_k^2\right)^2 P(k)$$

Redshift-space distortions

- We observe the distribution of galaxies

$$\delta_{\rm g} = b\delta_{\rm m} \qquad\qquad \mathbf{v}_{\rm g} = \mathbf{v}_{\rm m}$$

- The redshift-space galaxy density is then

$$\begin{aligned}\delta_{\rm g}^{\rm s}(\mathbf{k}) &= \delta_{\rm g}(\mathbf{k}) + \delta_{\rm m}(\mathbf{k}) f(z)\mu_k^2 \\ &= \delta_{\rm g}(\mathbf{k})\left(1+\beta(z)\mu_k^2\right)\end{aligned}$$

where $\beta(z) = \dfrac{f(z)}{b}$

- The galaxy power spectrum is given by

$$P_{\rm g}^{\rm s}(k,\mu_k) = b^2\left(1+\beta(z)\mu_k^2\right)^2 P_{\rm m}(k)$$

- This result can also be expressed as

$$P_{\rm g}^{\rm s}(k,\mu_k) = \left(b\sigma_8(z) + f\sigma_8(z)\mu_k^2\right)^2\left(\frac{P_{\rm m}(k,z)}{\sigma_8^2(z)}\right)$$

Legendre multipoles

- Decompose the power spectrum into Legendre multipoles

$$P_{\mathrm{g}}^{\mathrm{s}}(k,\mu_k) = \sum_{\ell\,\mathrm{even}} P_\ell(k)\, L_\ell(\mu_k)$$

$$P_\ell(k) = \frac{(2\ell+1)}{2}\int_{-1}^{1} P\left(k,\mu_k\right) L_\ell(\mu_k)\mathrm{d}\mu_k$$

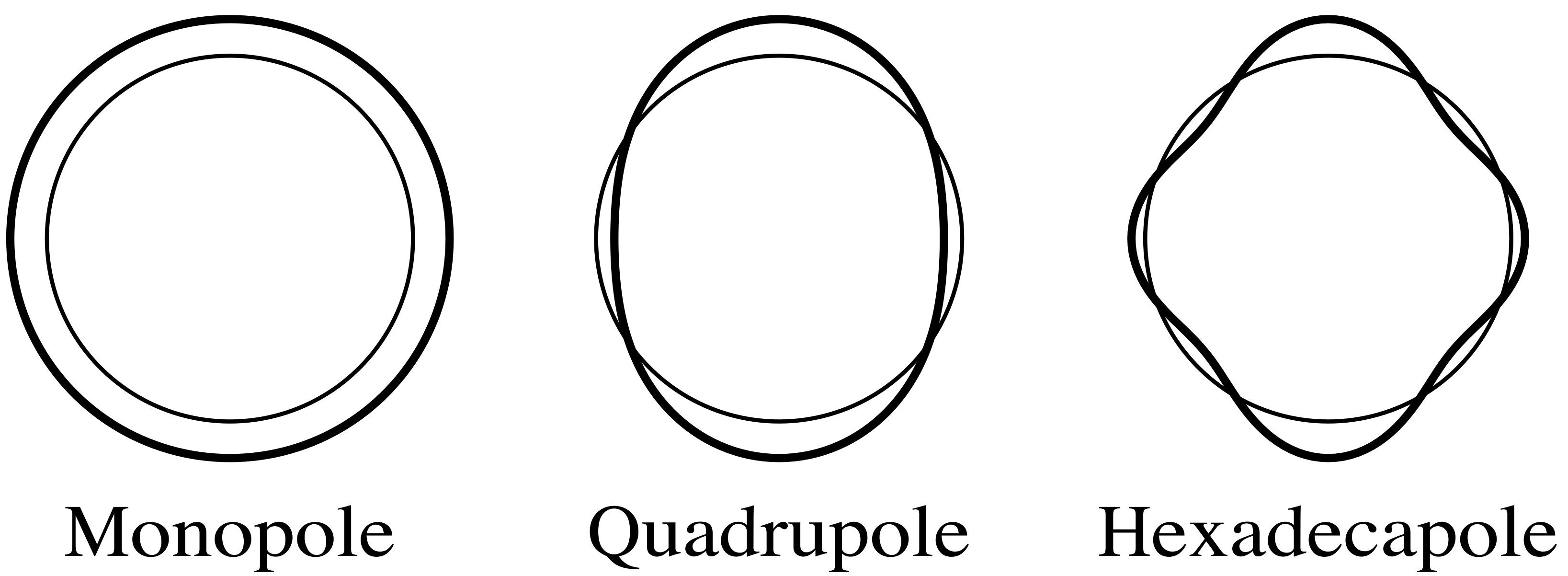

Legendre multipoles

- Decompose the power spectrum into Legendre multipoles

$$P_{\rm g}^{\rm s}(k,\mu_k) = \sum_{\ell\,{\rm even}} P_\ell(k)\, L_\ell(\mu_k)$$

$$P_\ell(k) = \frac{(2\ell+1)}{2}\int_{-1}^{1} P\left(k,\mu_k\right) L_\ell(\mu_k){\rm d}\mu_k$$

- In linear theory, only multipoles with $\ell > 4$ survive:

$$\frac{P_{\rm g}^{\rm s}(k,\mu_k)}{P_{\rm g}(k)} = \left(1+\frac{2}{3}\beta+\frac{1}{5}\beta^2\right) L_0(\mu) + \left(\frac{4}{3}\beta+\frac{4}{7}\beta^2\right) L_2(\mu) + \frac{8}{35}\beta^2\, L_4(\mu)$$

Legendre multipoles

- The Legendre multipoles in config.-space are given by

$$\xi_\ell(s) = \frac{i^\ell}{2\pi^2}\int_0^\infty P_\ell(k) j_\ell(ks) k^2\,\mathrm{d}k$$

leading to (Hamilton 1998):

$$\xi_0(s) = \left(1 + \frac{2}{3}\beta + \frac{1}{5}\beta^2\right)\xi(s),$$

$$\xi_2(s) = \left(\frac{4}{3}\beta + \frac{4}{7}\beta^2\right)\left(\xi(s) - \bar{\xi}(s)\right)$$

$$\xi_4(s) = \frac{8}{35}\beta^2\left(\xi(s) + \bar{\xi}(s) - \frac{7}{2}\bar{\bar{\xi}}(s)\right)$$

where:

$$\bar{\xi}(s) = \frac{3}{s^3}\int_0^s \xi(s')s'^2\,\mathrm{d}s',$$

$$\bar{\bar{\xi}}(s) = \frac{5}{s^5}\int_0^s \xi(s')s'^4\,\mathrm{d}s'$$

The non-linear regime

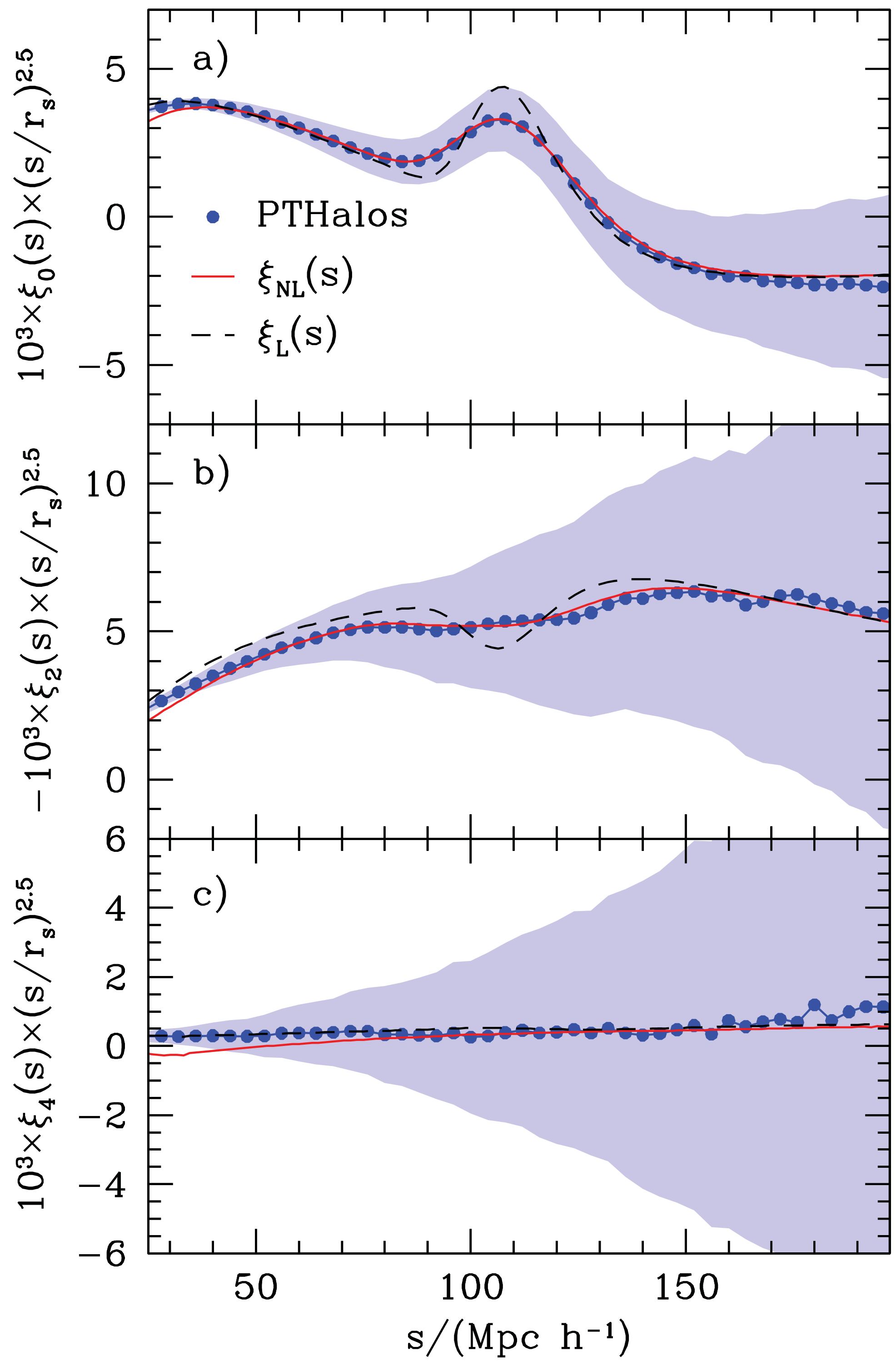

Sánchez et al. (2014)

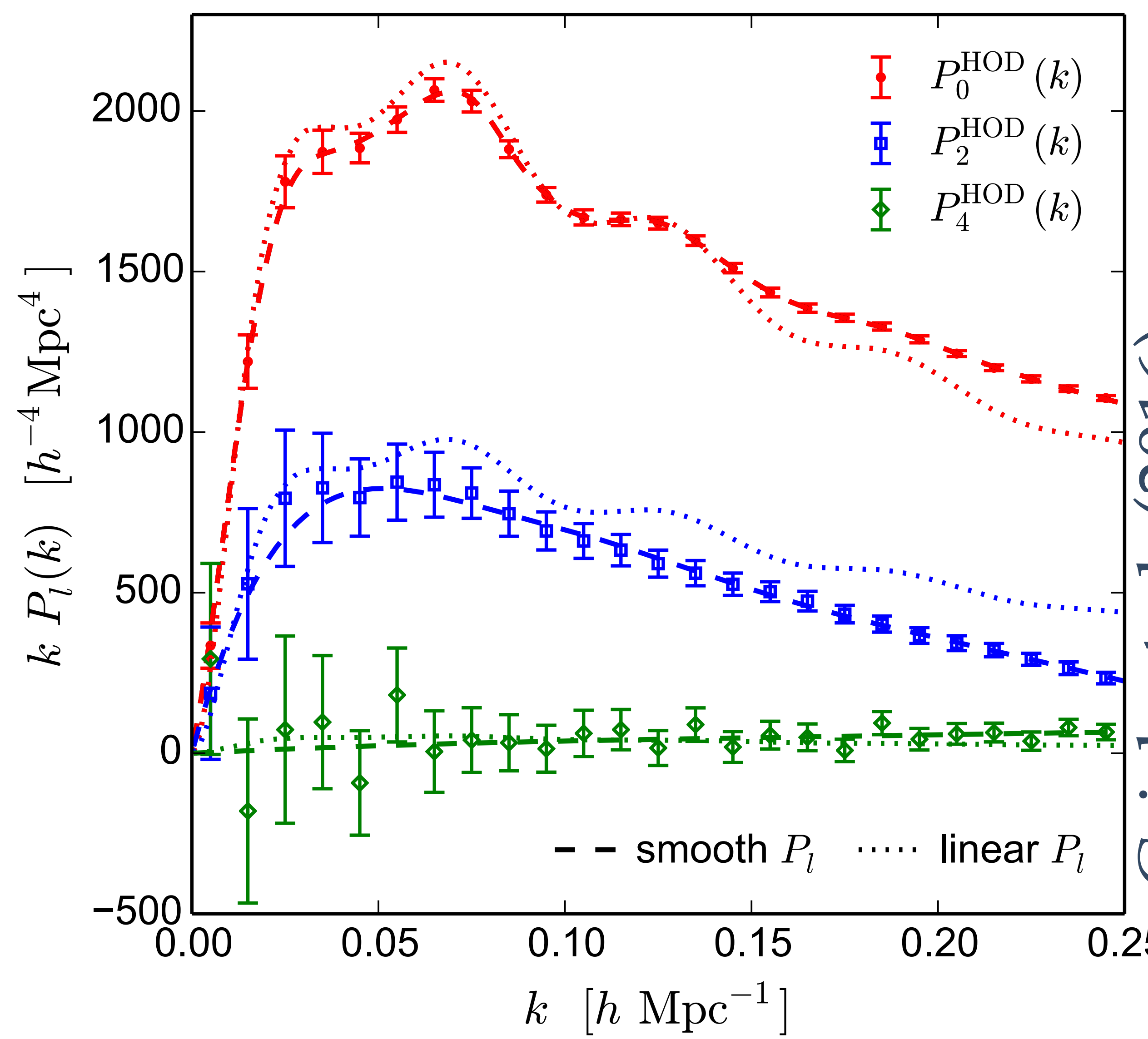

Grieb et al. (2016)

The non-linear regime

- RSD deviate from linear theory predictions even at high *z*.
- High-density peaks are characterised by large velocity dispersions -> the *figers-of-God* effect.

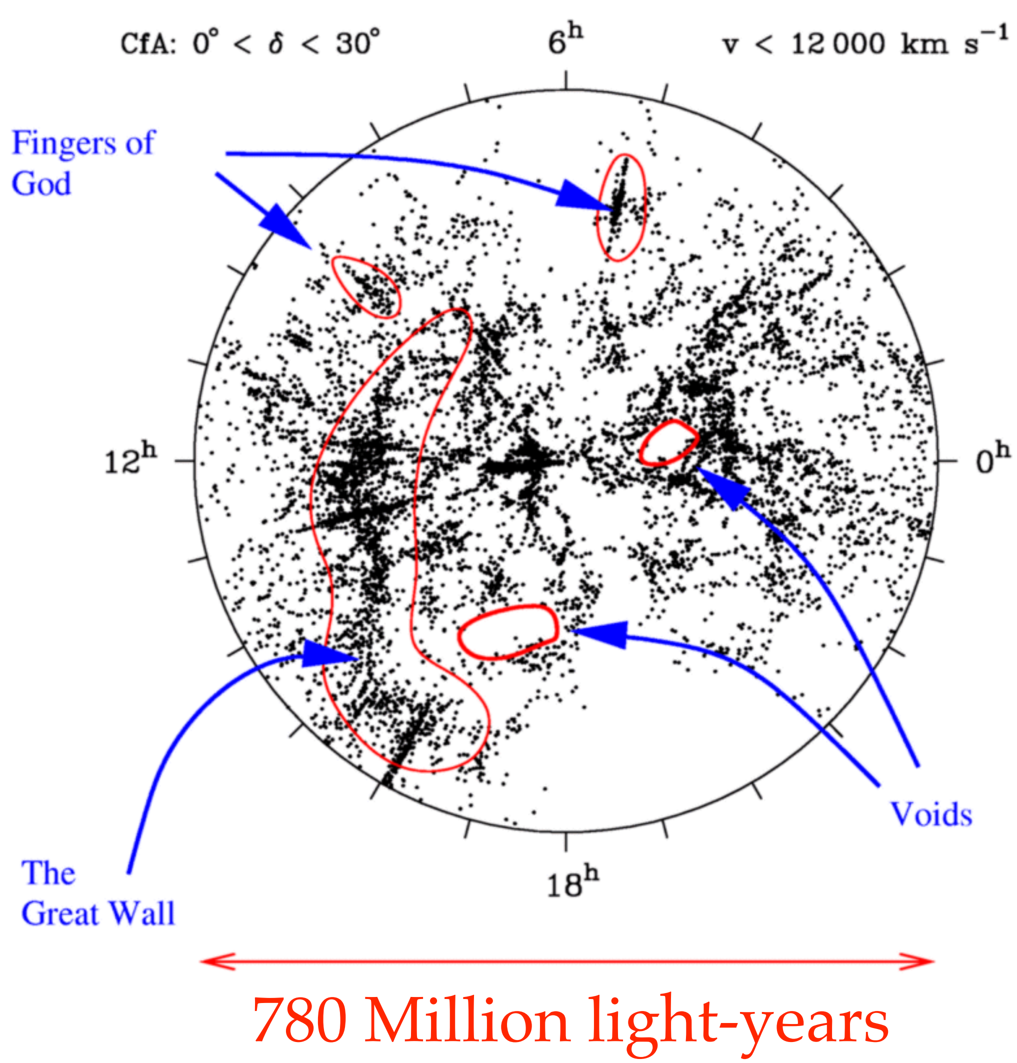

The non-linear regime

- RSD deviate from linear theory predictions even at high z.
- High-density peaks are characterised by large velocity dispersions -> the *figers-of-God* effect.
- The non-linear power spectrum is often described as

$$P(k,\mu) = W_\infty(ifk\mu)\,P_{\mathrm{novir}}(k,\mu),$$

Non-linear corrections associated with virialized regions

Coherent flow towards high-density regions.

Modelling BAO & RSD

- Cosmological analysis of the final BOSS (Sánchez et al. 2017, Grieb et al. 2017, Salazar-Albornoz 2017)

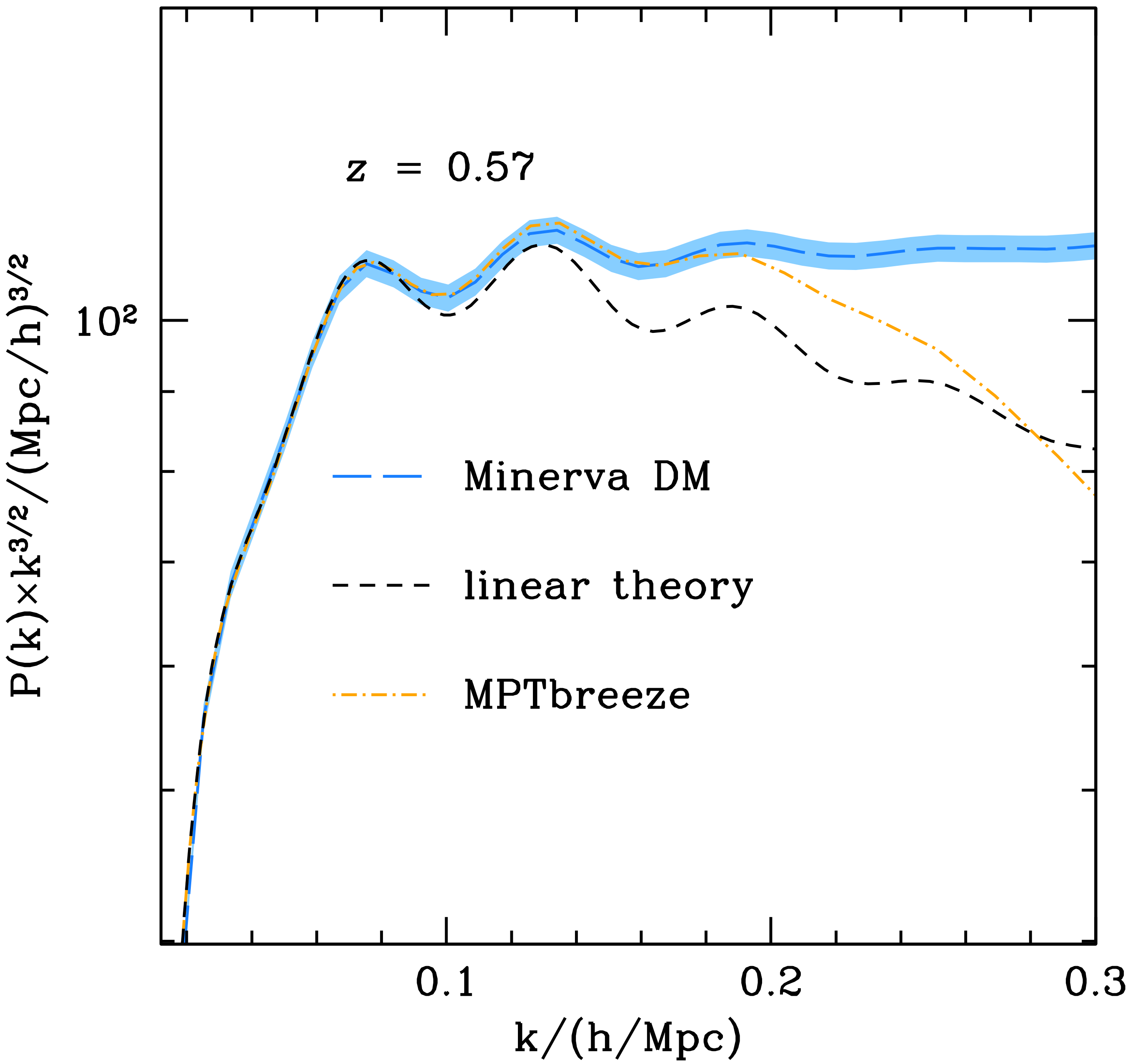

Modelling BAO & RSD

- Cosmological analysis of the final BOSS (Sánchez et al. 2017, Grieb et al. 2017, Salazar-Albornoz 2017)

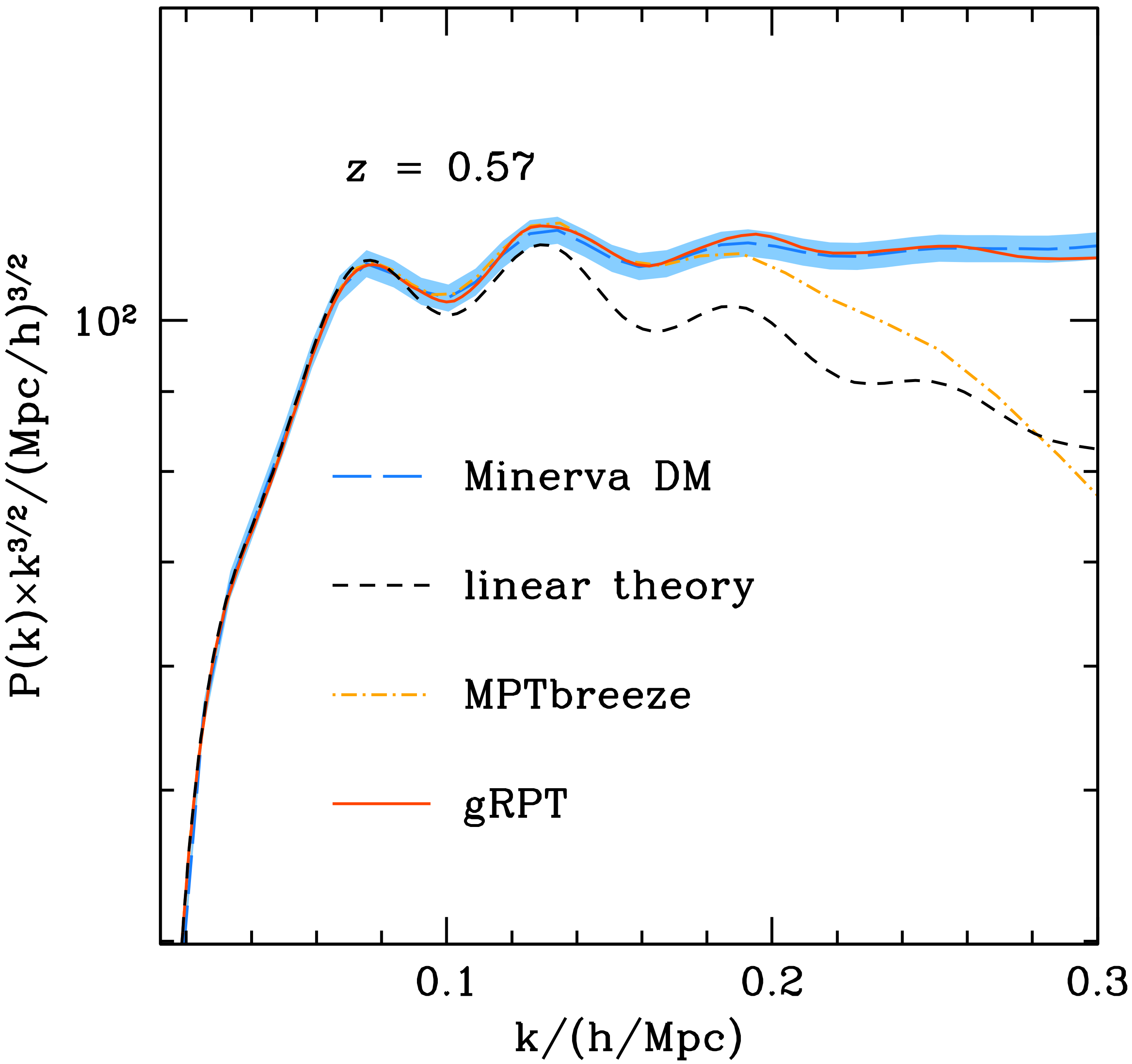

Modelling BAO & RSD

- We describe galaxy bias as (Chan et al. 2012)

$$\delta_{\rm g} = b_1\delta + \frac{b_2}{2}\delta^2 + \gamma_2\,\mathcal{G}_2 + \gamma_3^-\,\Delta_3\mathcal{G} + \ldots$$

where

$$\mathcal{G}_2(\Phi_v) = (\nabla_{ij}\Phi_v)^2 - (\nabla^2\Phi_v)^2,$$

$$\Delta_3\mathcal{G} = \mathcal{G}_2(\Phi) - \mathcal{G}_2(\Phi_v),$$

- We model the FoG factor as

$$W_\infty(\lambda) = \frac{1}{\sqrt{1-\lambda^2 a_{\rm vir}^2}}\exp\left(\frac{\lambda^2\sigma_v^2}{1-\lambda^2 a_{\rm vir}^2}\right),$$

Modelling BAO & RSD

- The *non-virial* power spectrum has three contributions

$$P^{(1)}_{\rm novir}(k,\mu) = P_{gg}(k) + 2f\mu^2 P_{g\theta}(k) + f^2\mu^4 P_{\theta\theta}(k)$$

$$P^{(2)}_{\rm novir}(k,\mu) = \int \frac{q_z}{q^2}\Big[B_{\theta D_s D_s}(\mathbf{q}, \mathbf{k}-\mathbf{q}, -\mathbf{k}) + B_{\theta D_s D_s}(\mathbf{q}, -\mathbf{k}, \mathbf{k}-\mathbf{q})\Big],$$

$$P^{(3)}_{\rm novir}(k,\mu) = \int \frac{q_z}{q^2}\frac{(k_z - q_z)}{(\mathbf{k}-\mathbf{q})^2}(b_1 + f\mu_q^2)(b_1 + f\mu_{k-q}^2) \times P_{\delta\theta}(k-q)P_{\delta\theta}(q)d^3q.$$

Anisotropic clustering

- BOSS anisotropic clustering measurements

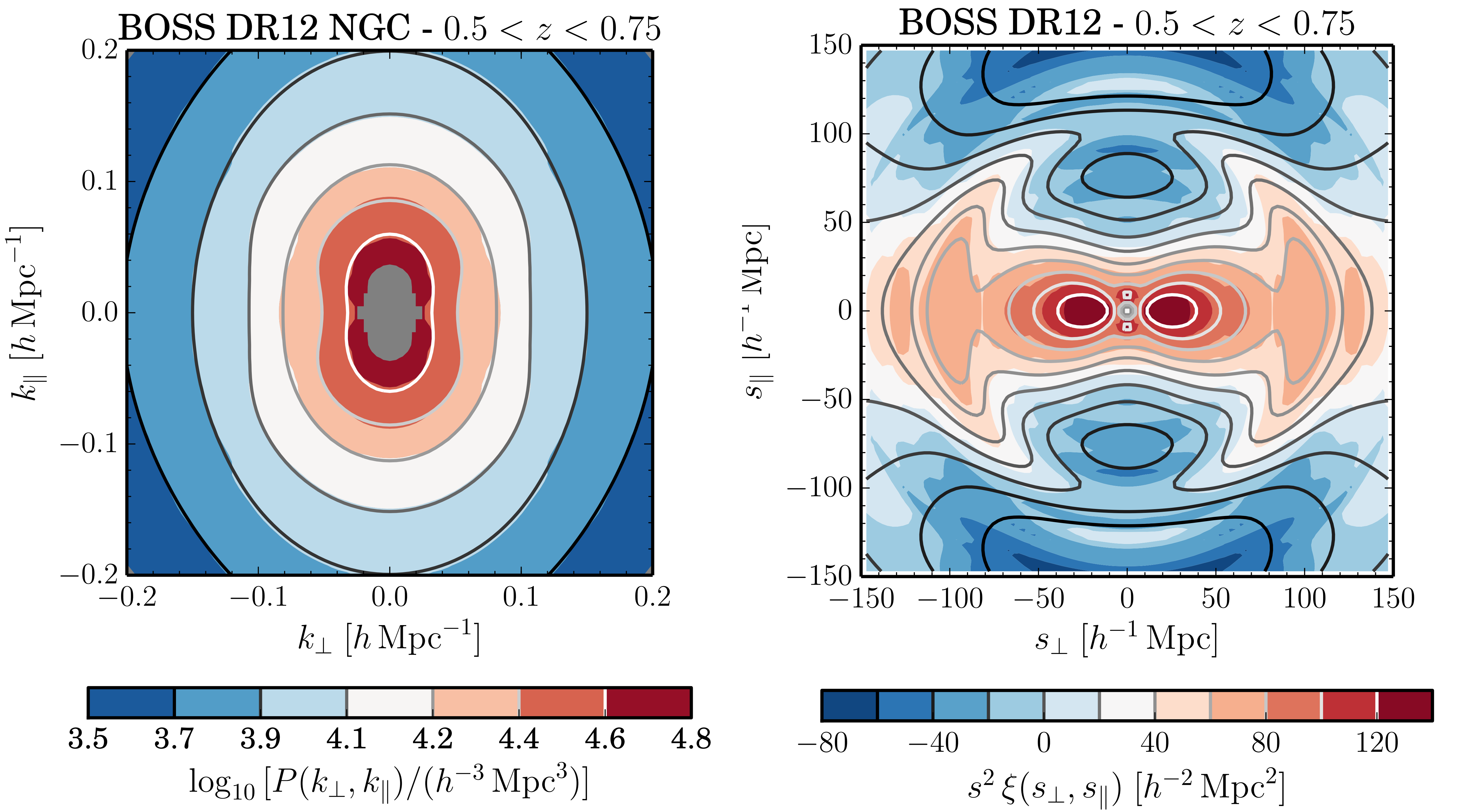

Anisotropic clustering

- Project $\xi(s_\perp, s_\parallel)$ into Legendre multipoles:

$$\xi_\ell(s) = \frac{(2\ell+1)}{2}\int_{-1}^{1}\xi(\mu,s)\,L_\ell(\mu)\,\mathrm{d}\mu$$

- Use clustering wedges (Kazin, Sánchez & Blanton, 2012).

$$\xi_{\mu_1}^{\mu_2} = \frac{1}{\mu_2-\mu_1}\int_{\mu_1}^{\mu_2}\xi(\mu,s)\mathrm{d}\mu$$

- In Fourier space:

$$P_\ell(k),\ \ P_{\mu_1}^{\mu_2}(k)$$

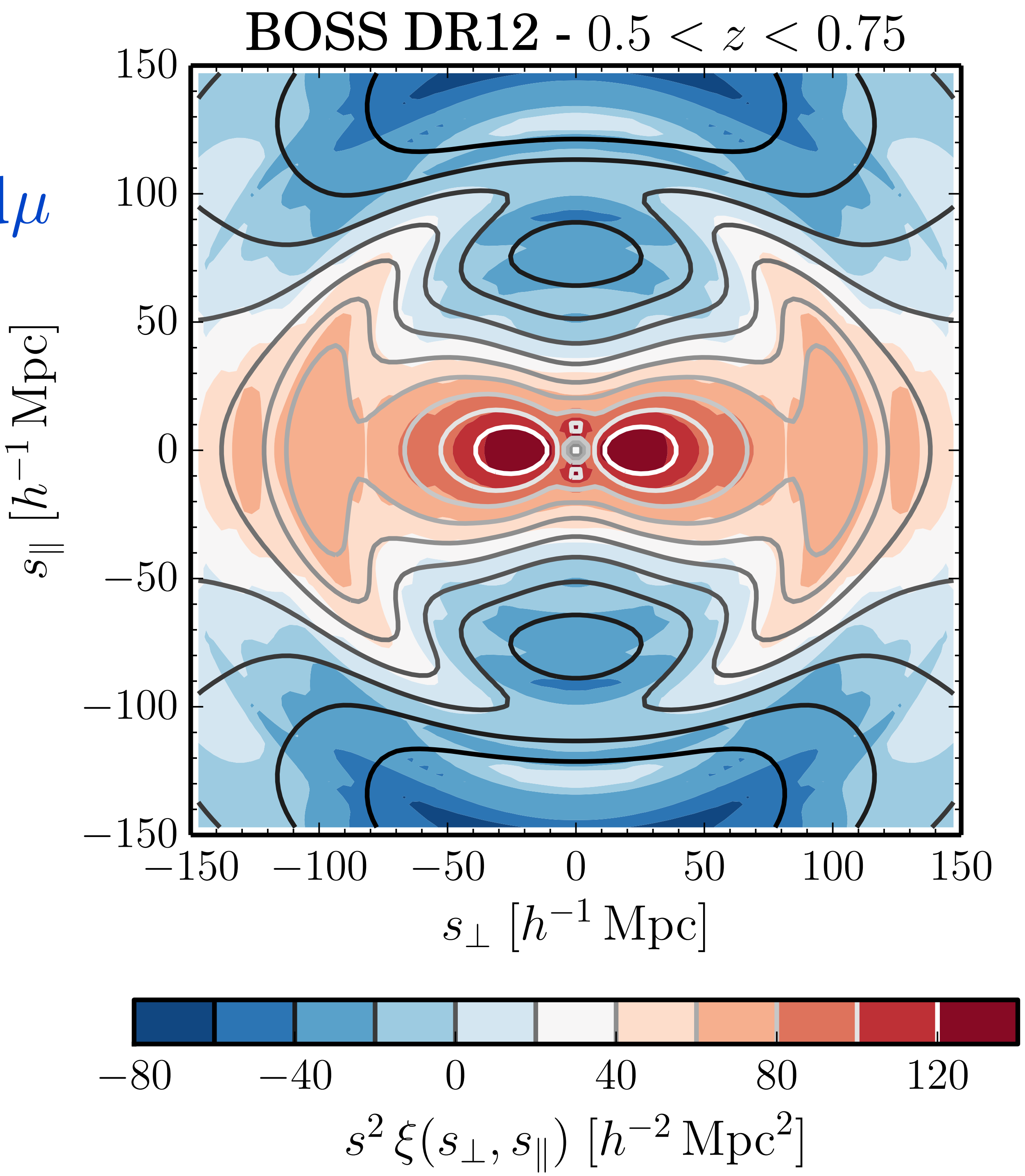

Anisotropic clustering

- Project $\xi(s_\perp, s_\parallel)$ into Legendre multipoles:

$$\xi_\ell(s) = \frac{(2\ell+1)}{2}\int_{-1}^{1}\xi(\mu,s)\,L_\ell(\mu)\,\mathrm{d}\mu$$

- Use clustering wedges (Kazin, Sánchez & Blanton, 2012).

$$\xi_{\mu_1}^{\mu_2} = \frac{1}{\mu_2-\mu_1}\int_{\mu_1}^{\mu_2}\xi(\mu,s)\mathrm{d}\mu$$

- In Fourier space:

$$P_\ell(k),\ \ P_{\mu_1}^{\mu_2}(k)$$

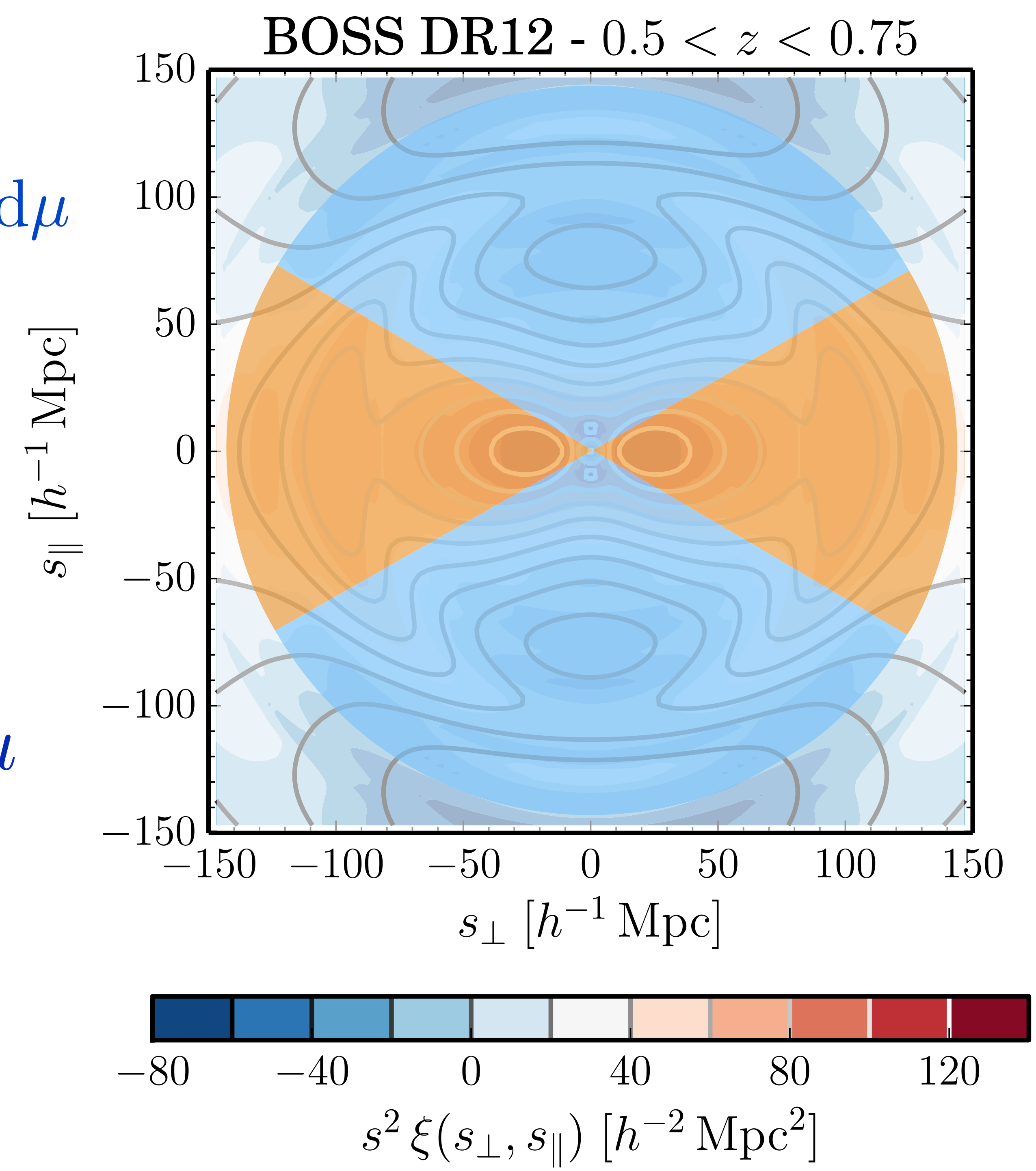

Anisotropic clustering

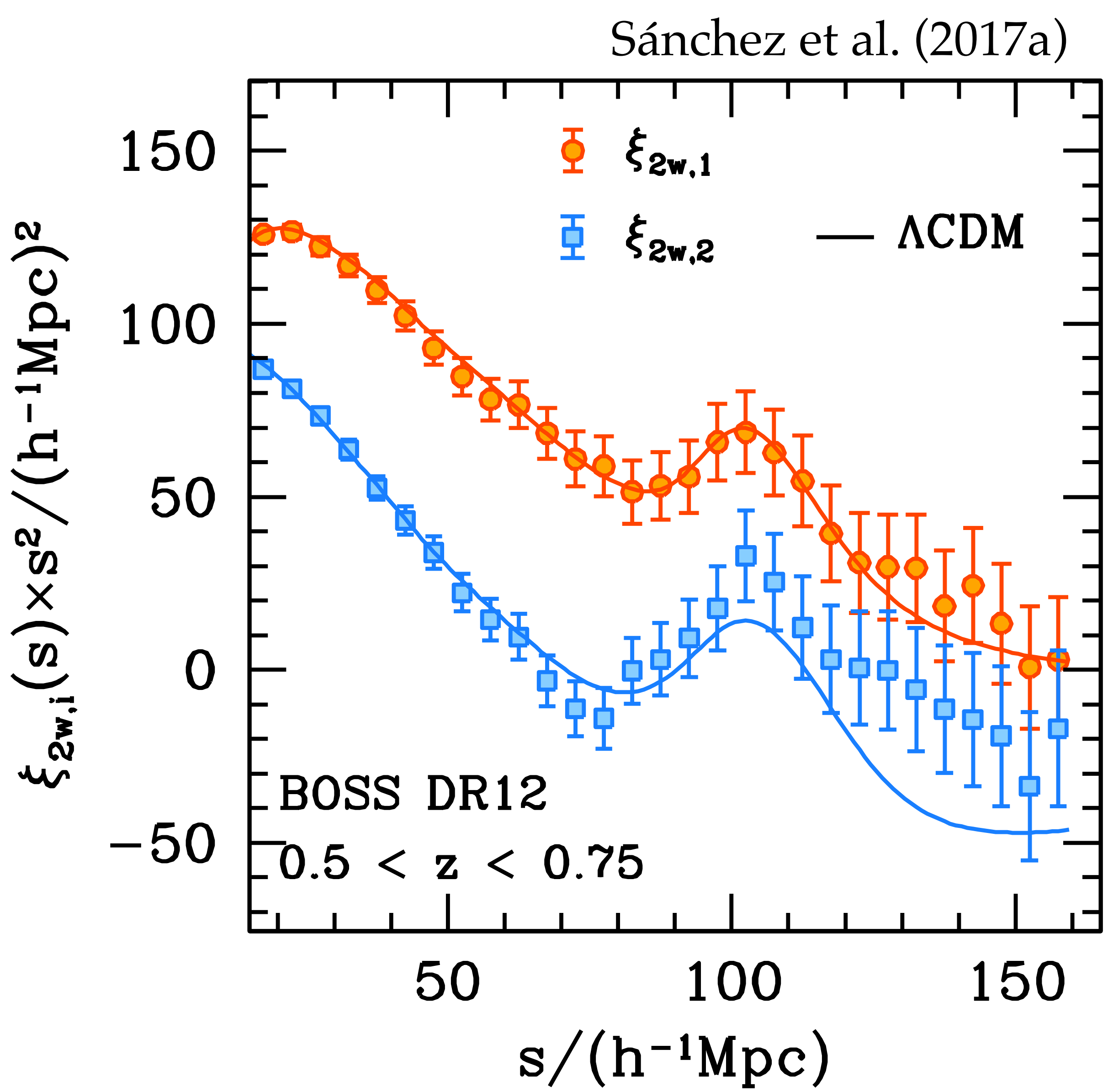

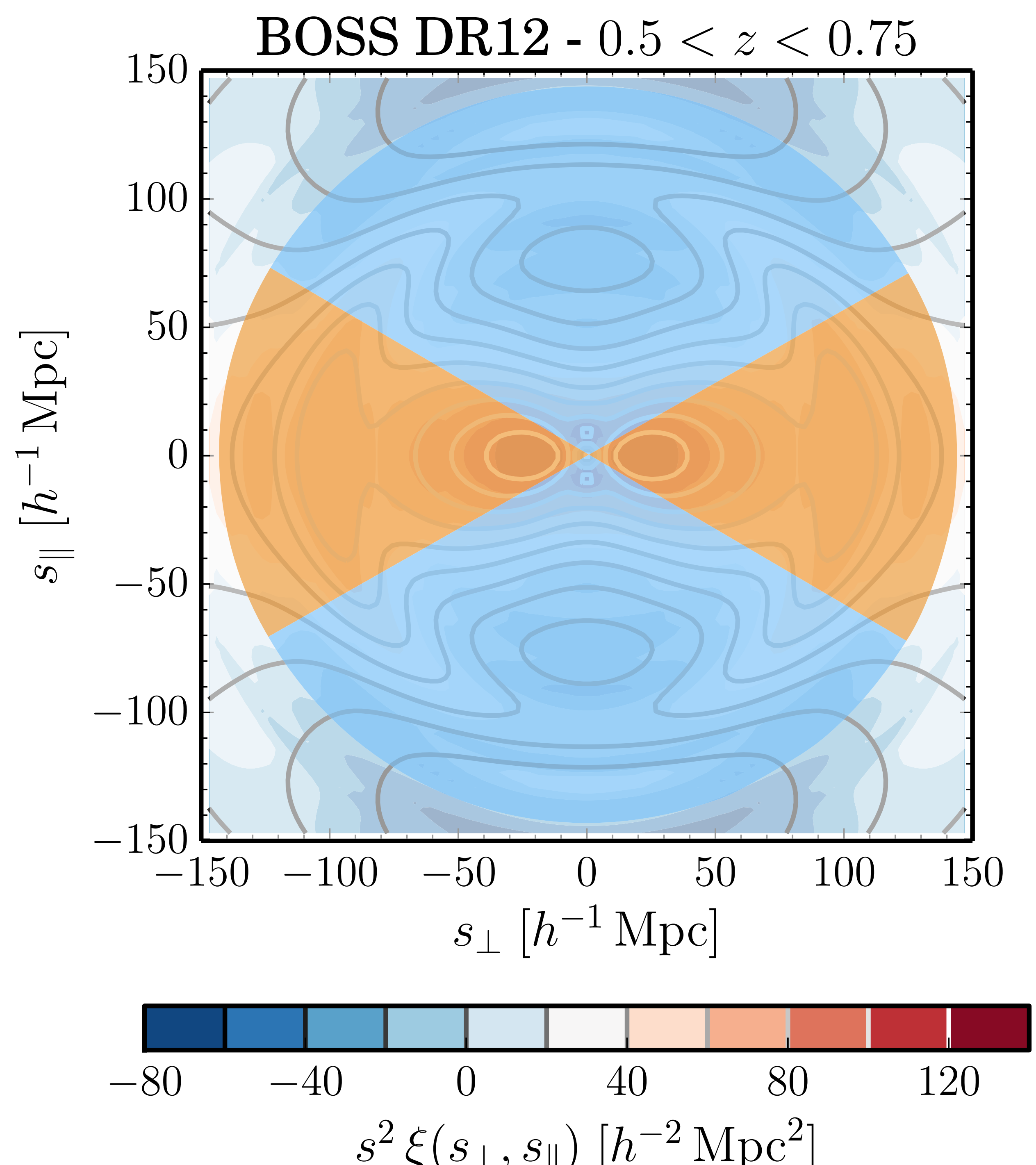

Anisotropic clustering

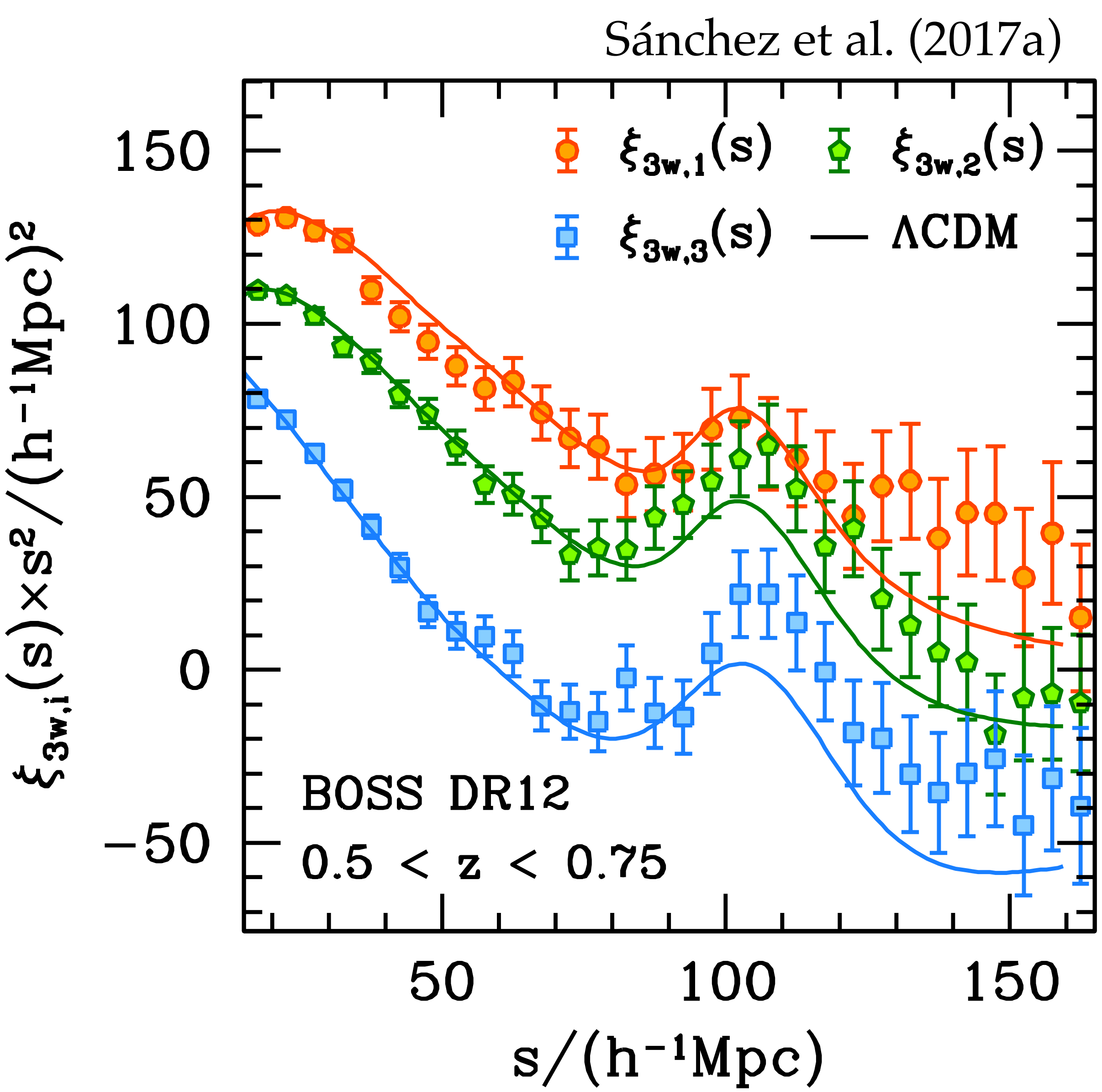

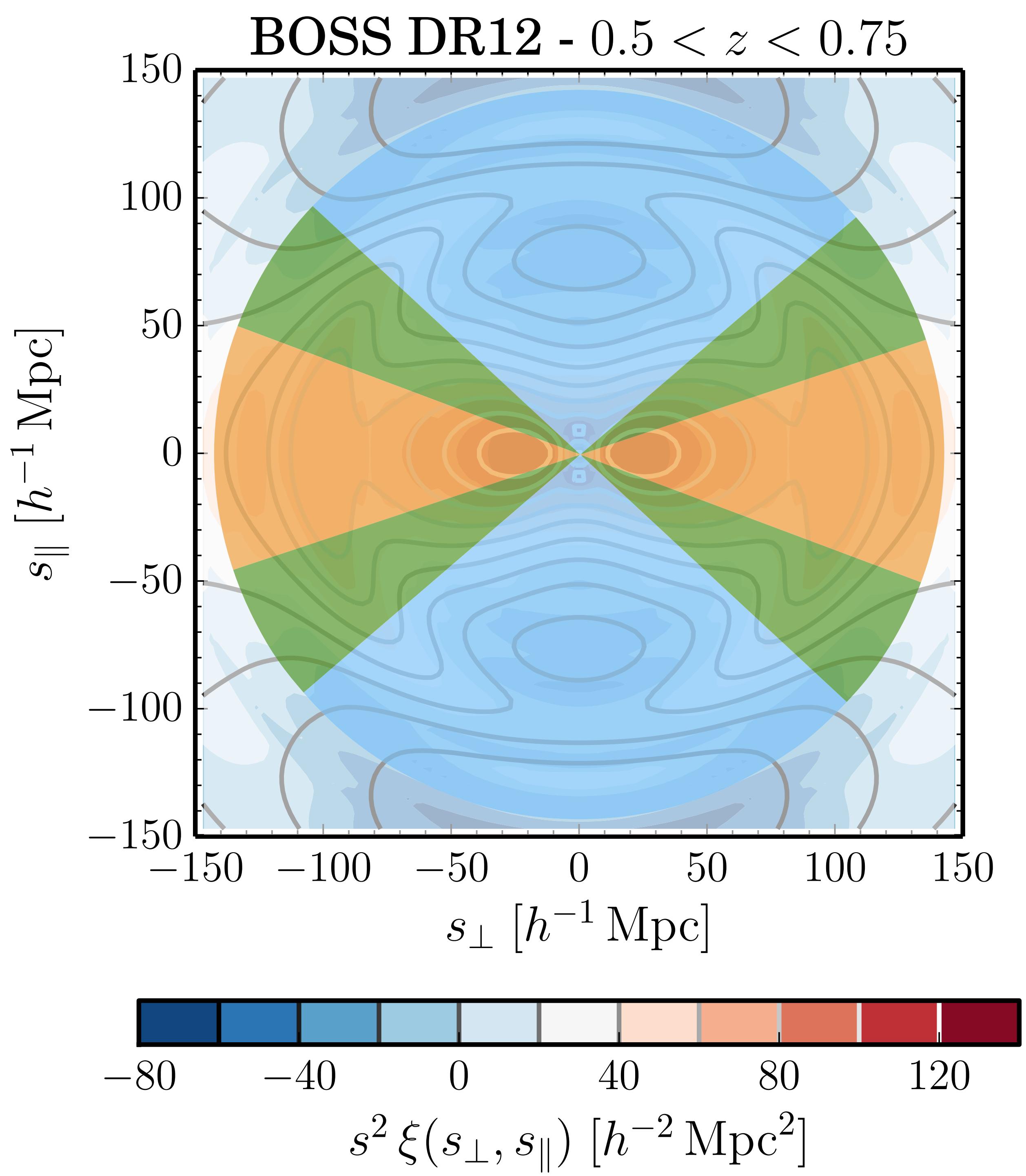

Anisotropic clustering

- BOSS DR12 clustering wedges:

Sánchez et al. (2017a)

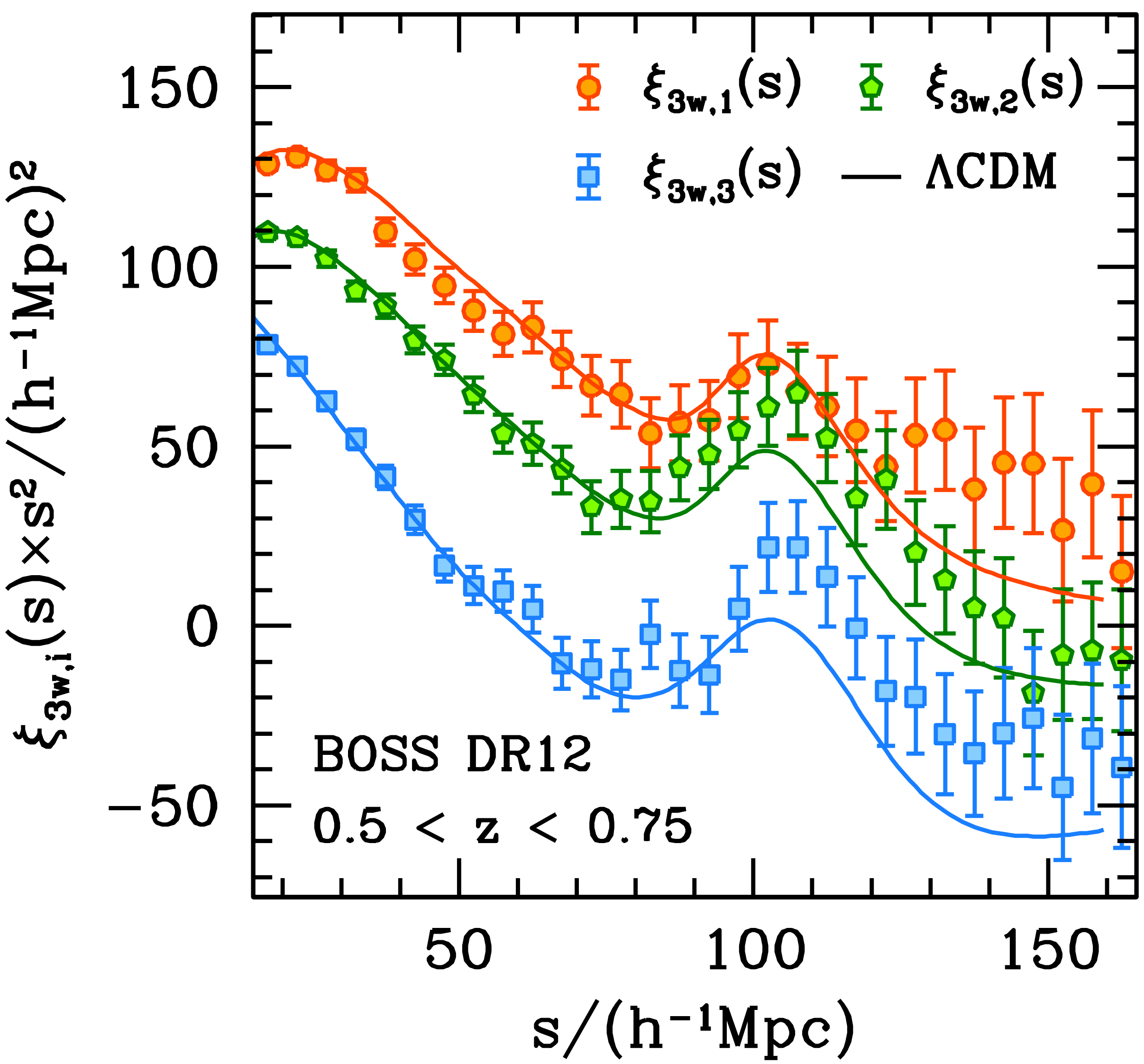

Grieb et al. (2017)

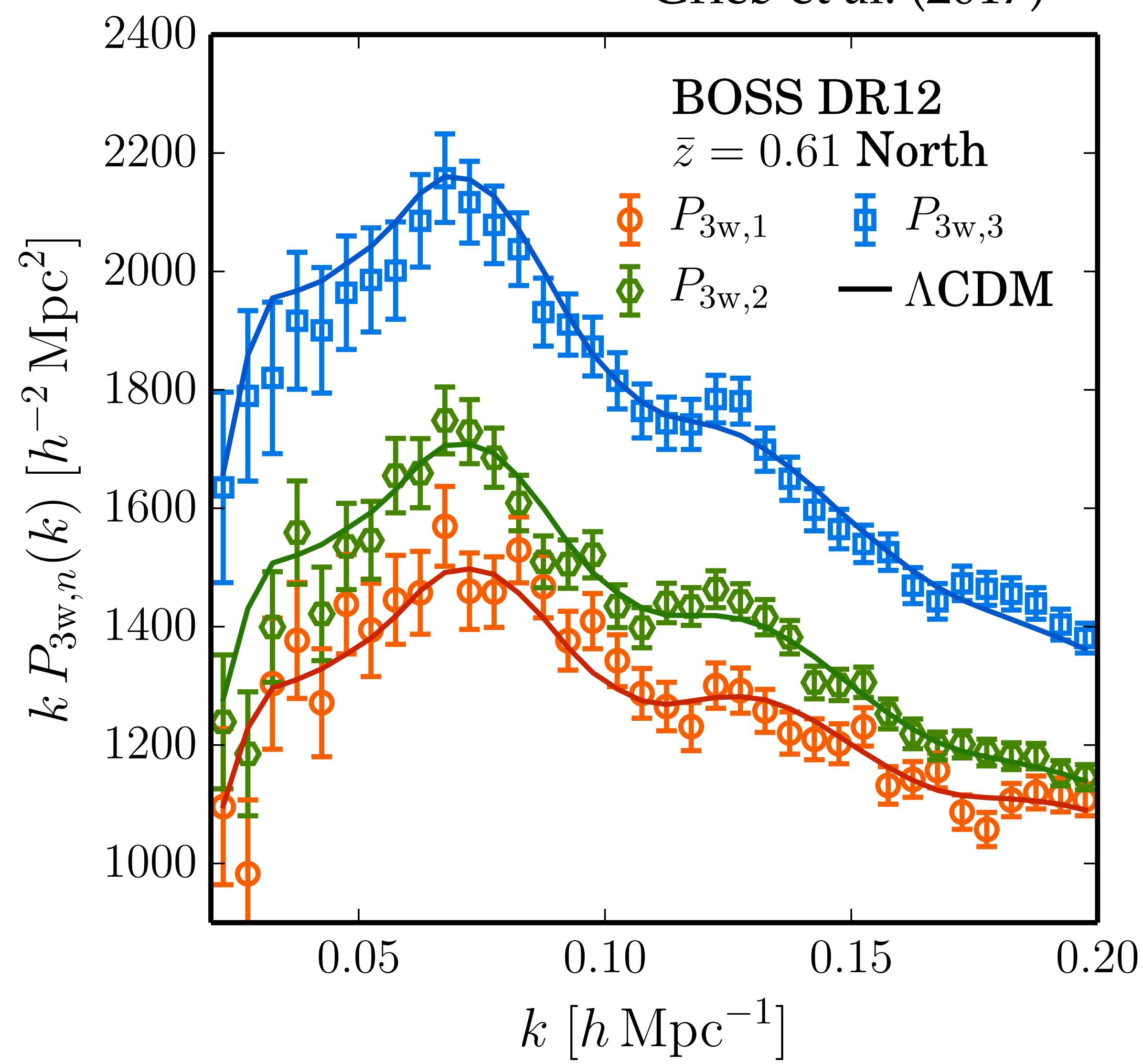

The growth rate of cosmic structure

Alam et al. (2017)

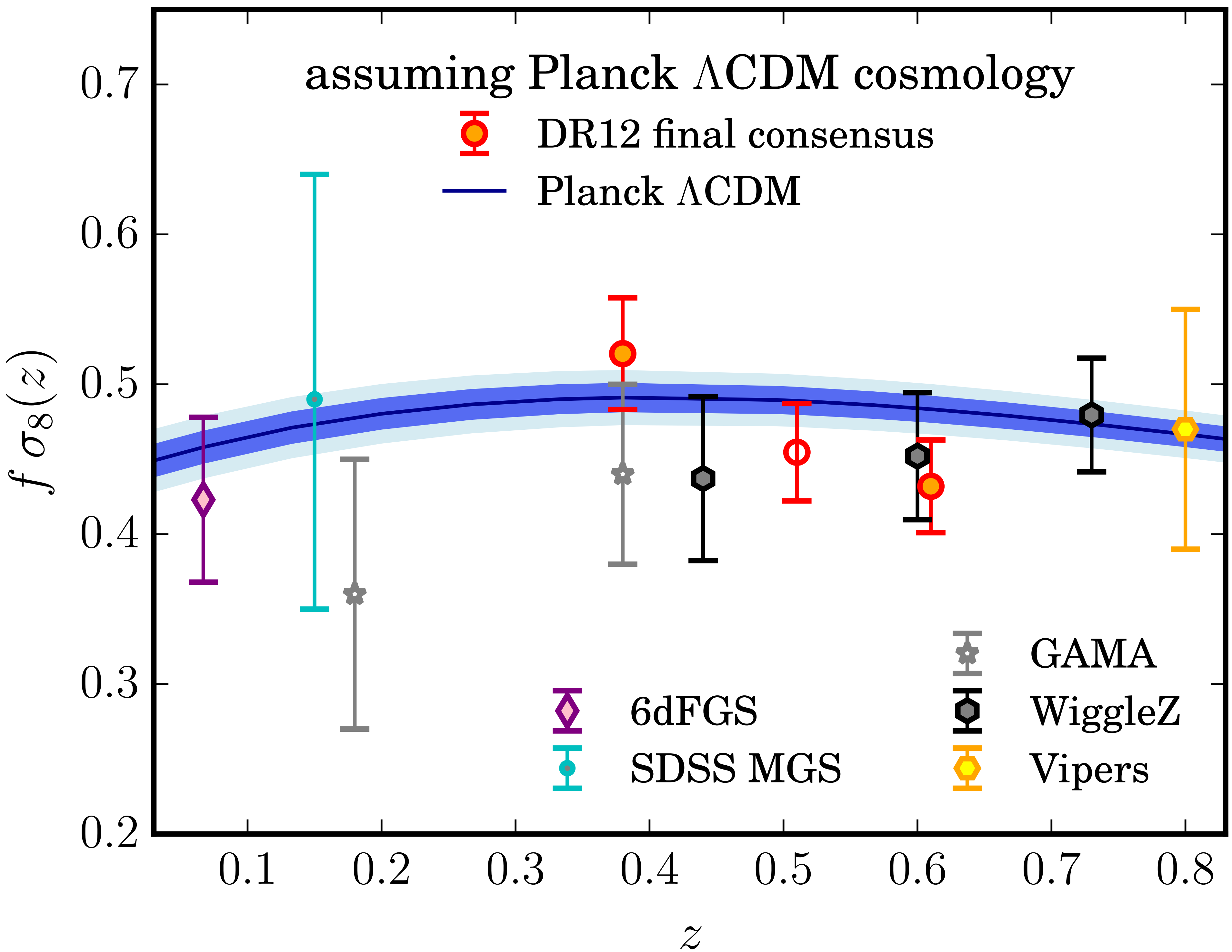

Cosmology from LSS observations

- Observational effects of cosmic acceleration:

  - Expansion history of the Universe:

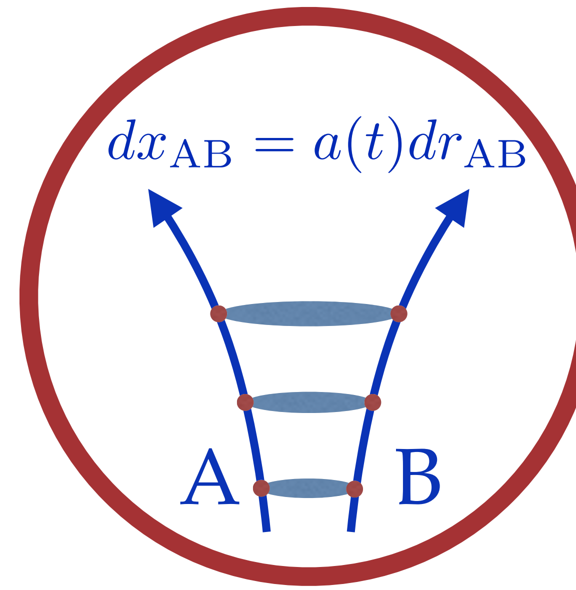

$$H(z) = \frac{\dot{a}}{a} \qquad r(z) = \int_0^z \frac{c\,dz'}{H(z')}$$

  - Growth of density fluctuations:

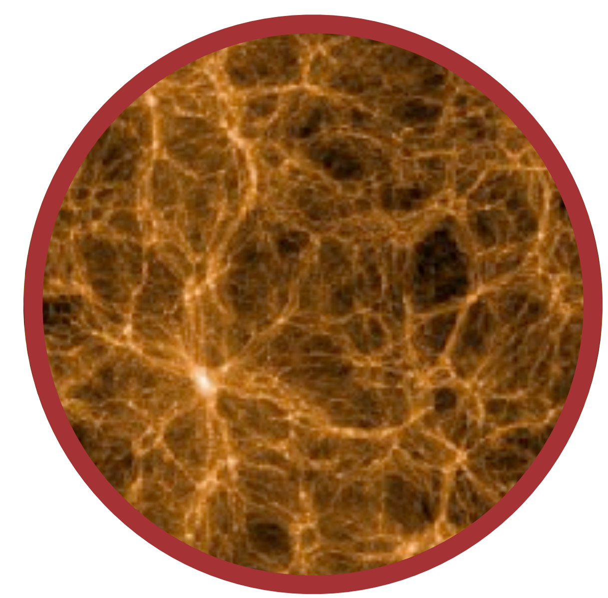

$$\delta = \frac{\rho - \bar{\rho}}{\bar{\rho}}$$

- Both effects can be probed by LSS observations

Full-shape clustering analyses

- Clustering measurements contain additional information beyond BAO.

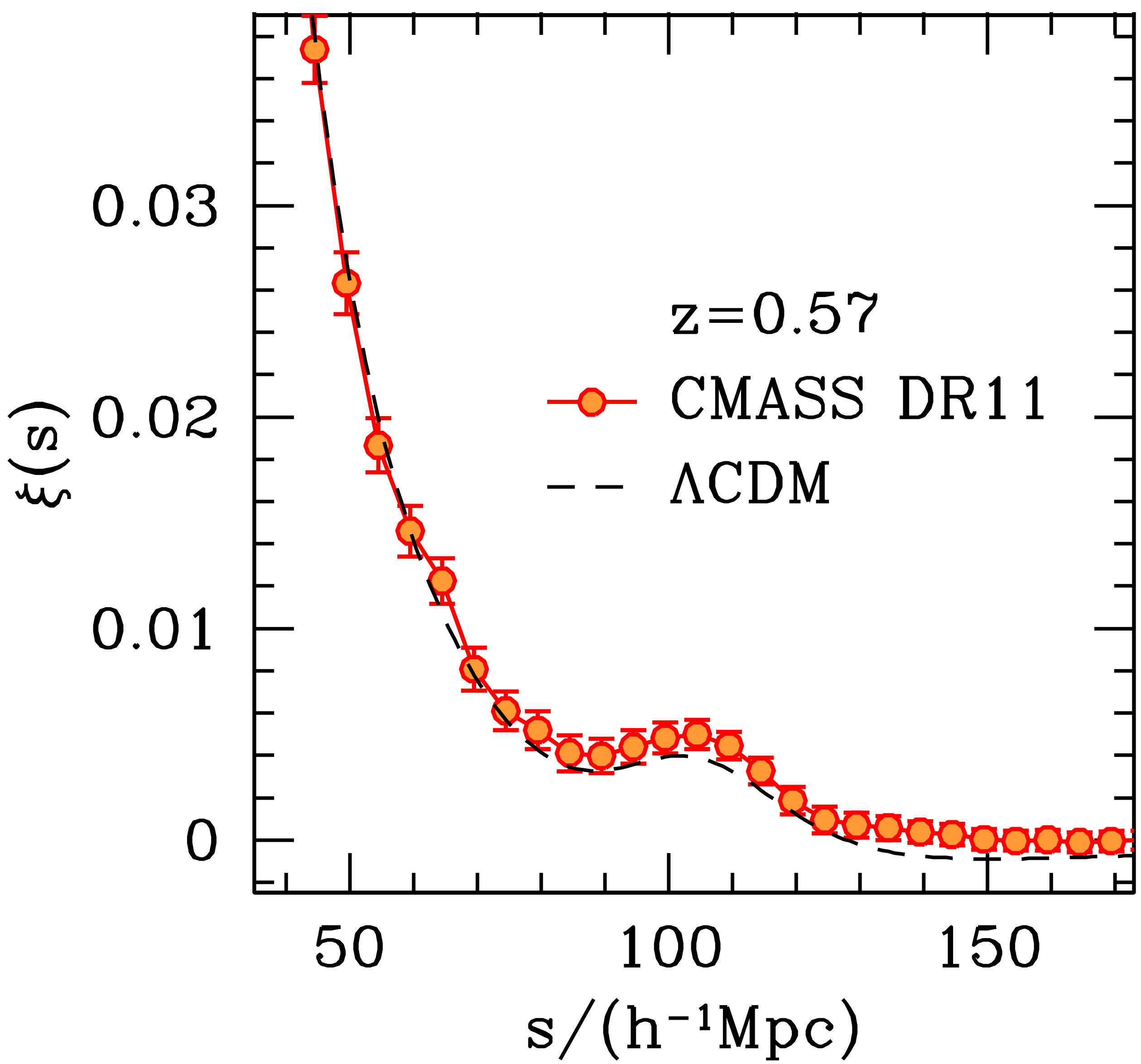

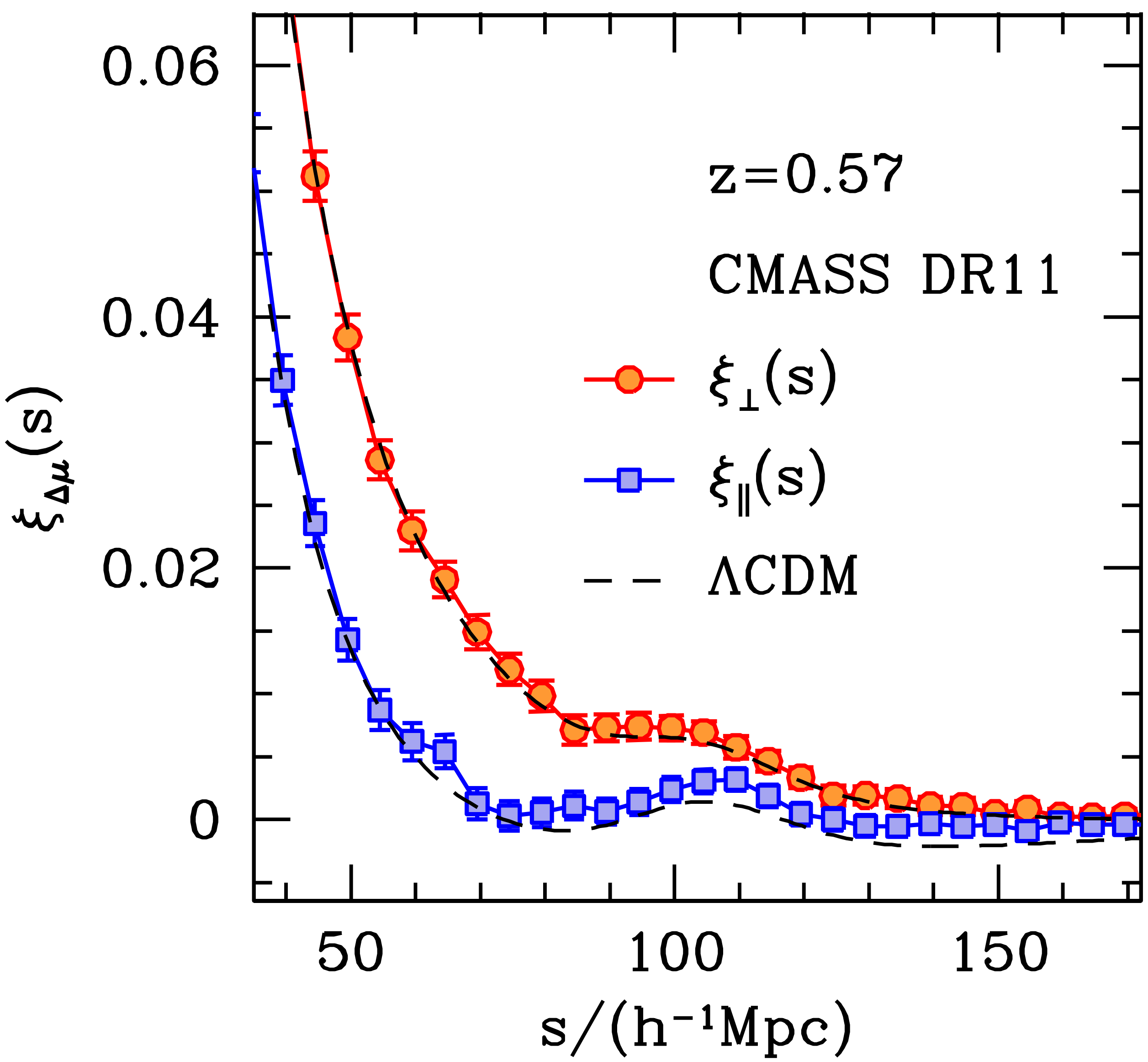

Sánchez et al.(2014)

The dark energy equation of state

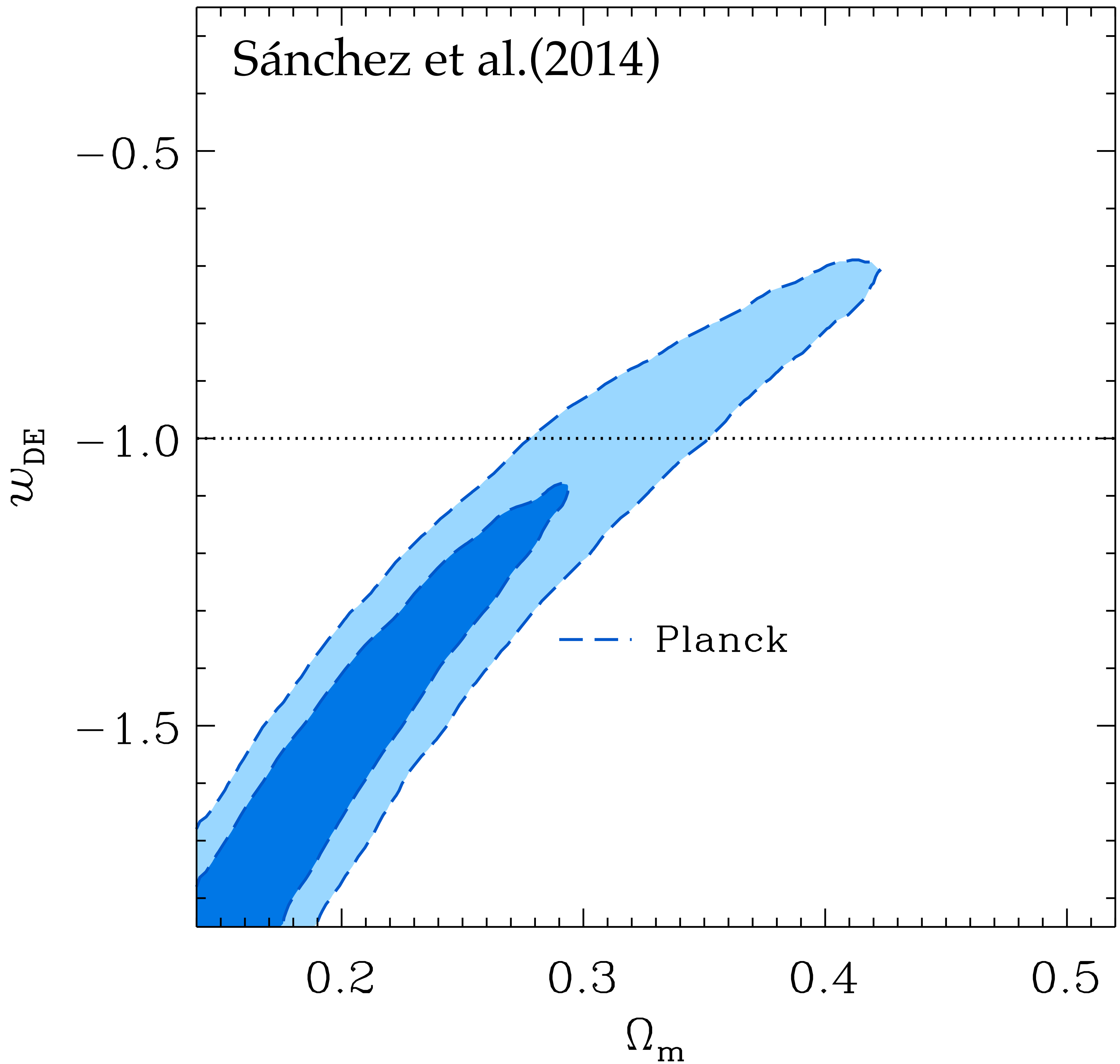

The dark energy equation of state

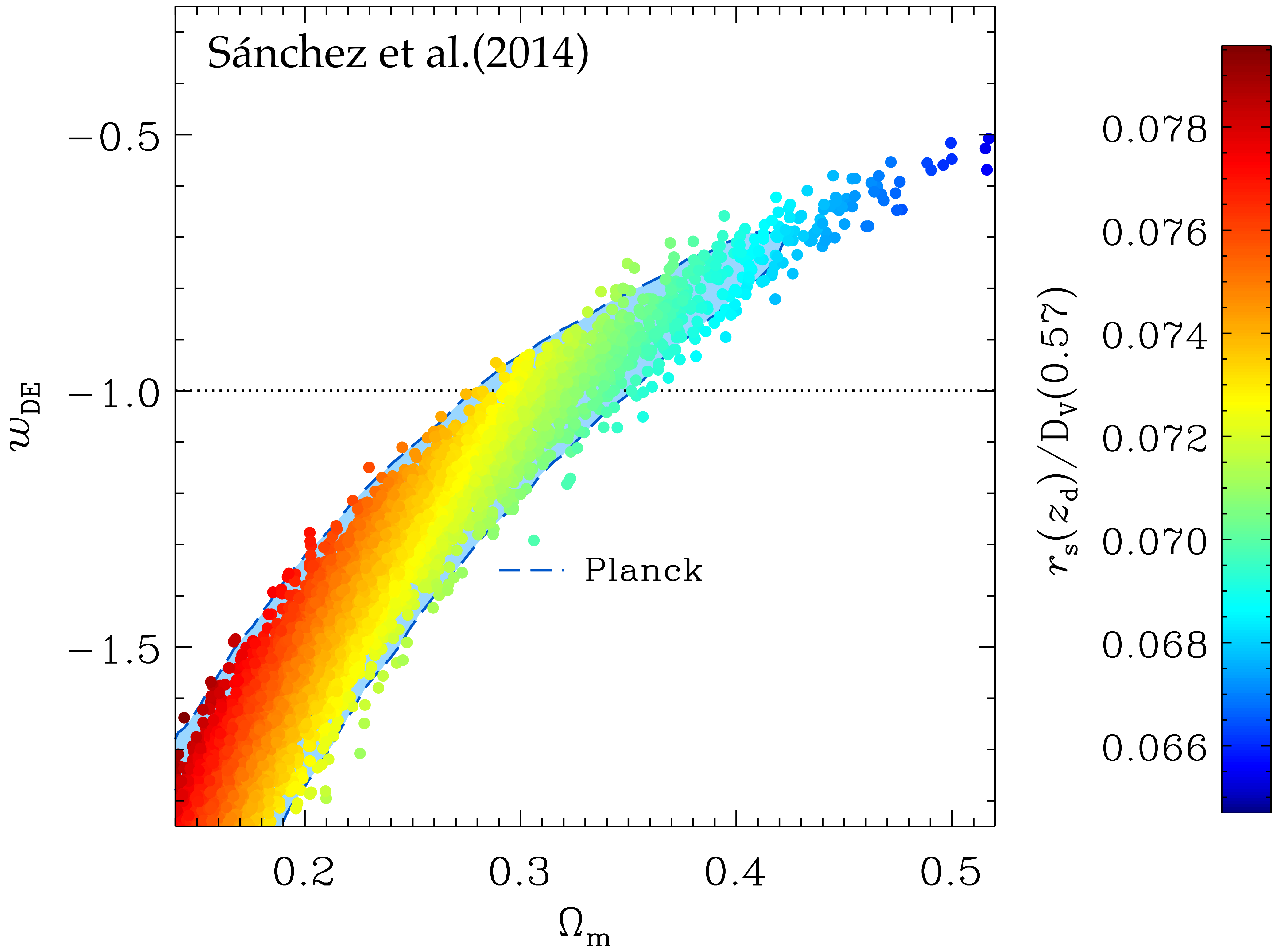

The dark energy equation of state

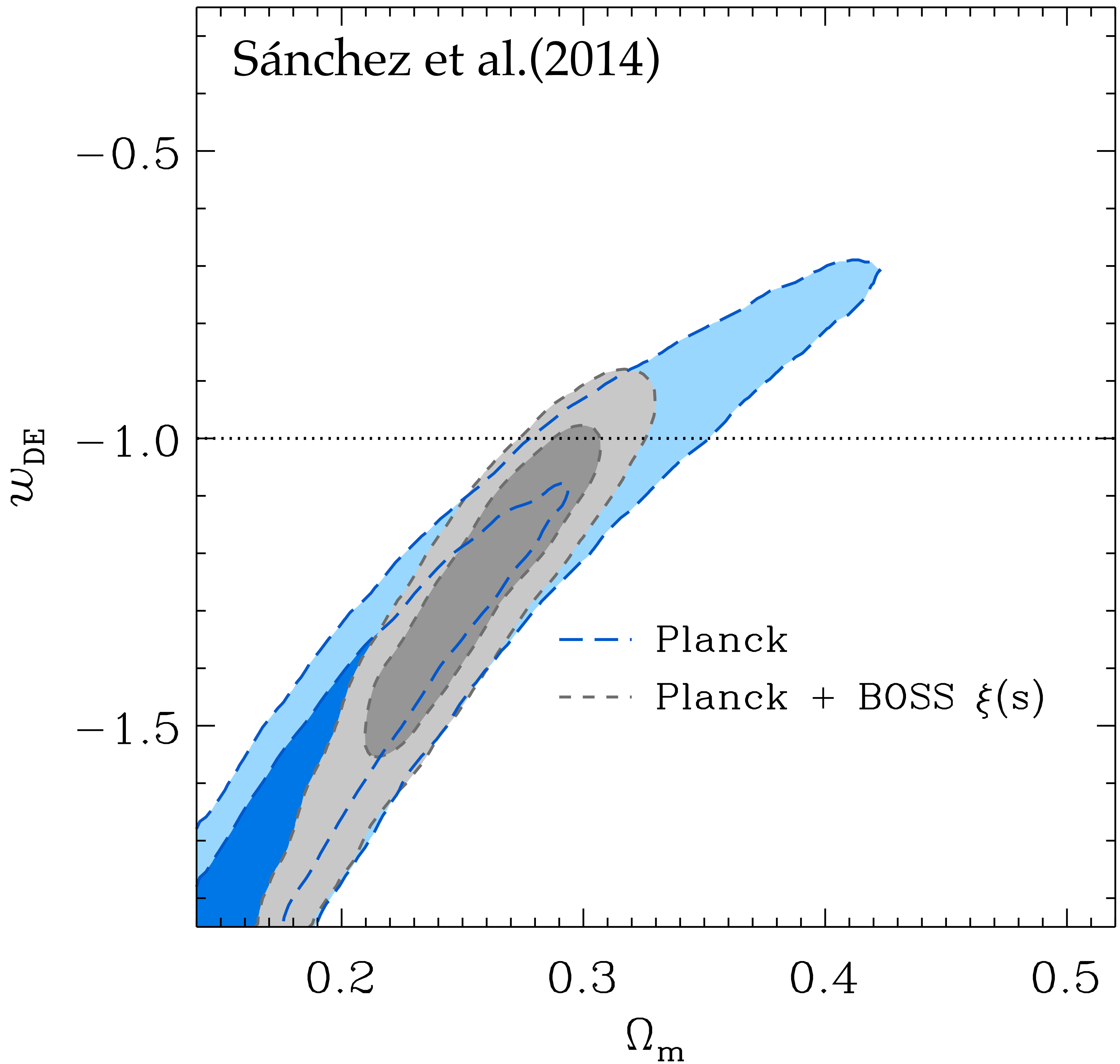

Planck + BOSS $\xi(s)$

$$\Omega_{\mathrm{m}} = 0.249^{+0.034}_{-0.026}$$

$$w_{\mathrm{DE}} = -1.31^{+0.21}_{-0.16}$$

The dark energy equation of state

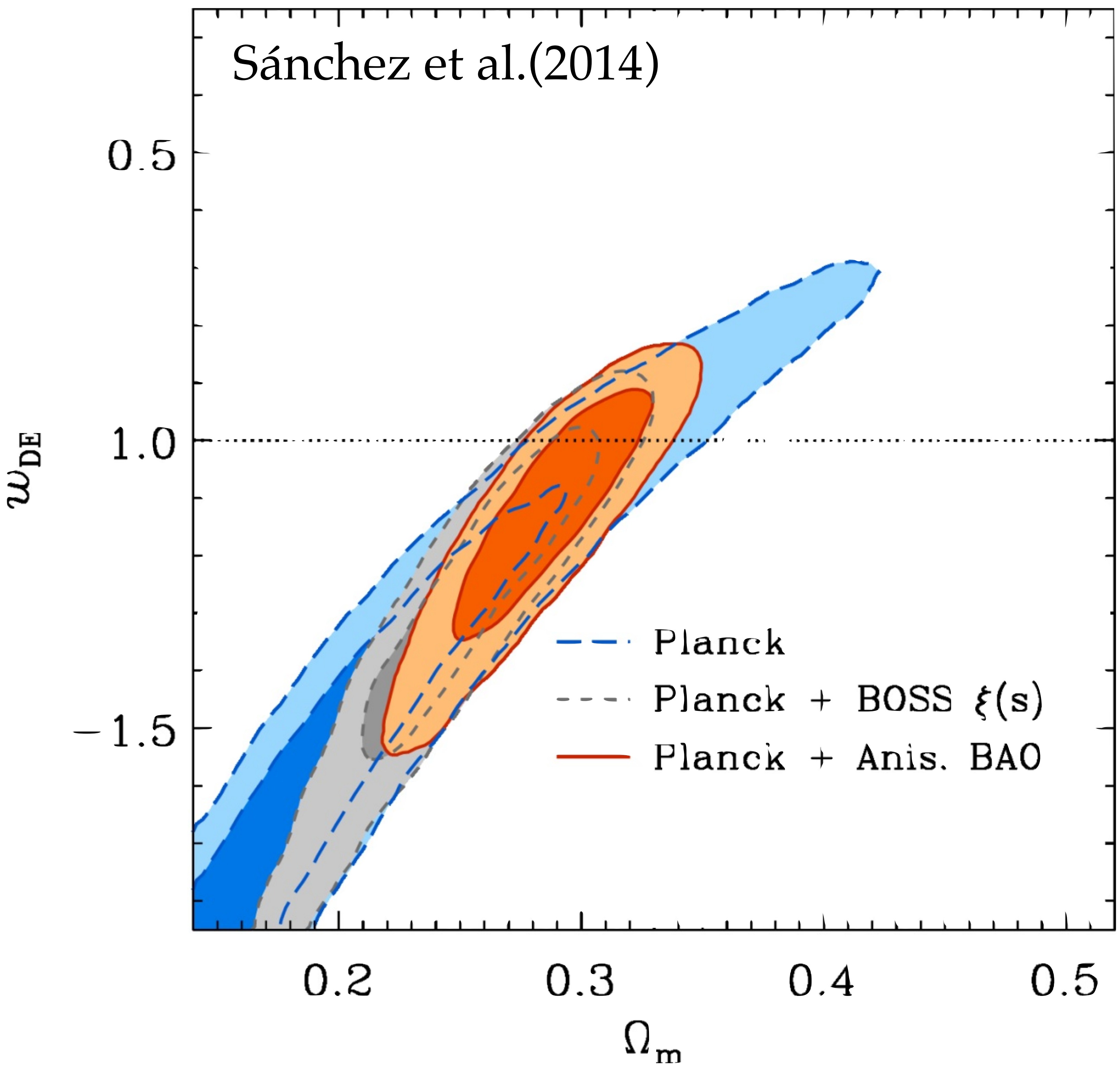

Planck + BOSS $\xi(s)$

$$\Omega_{\rm m} = 0.249^{+0.034}_{-0.026}$$

$$w_{\rm DE} = -1.31^{+0.21}_{-0.16}$$

The dark energy equation of state

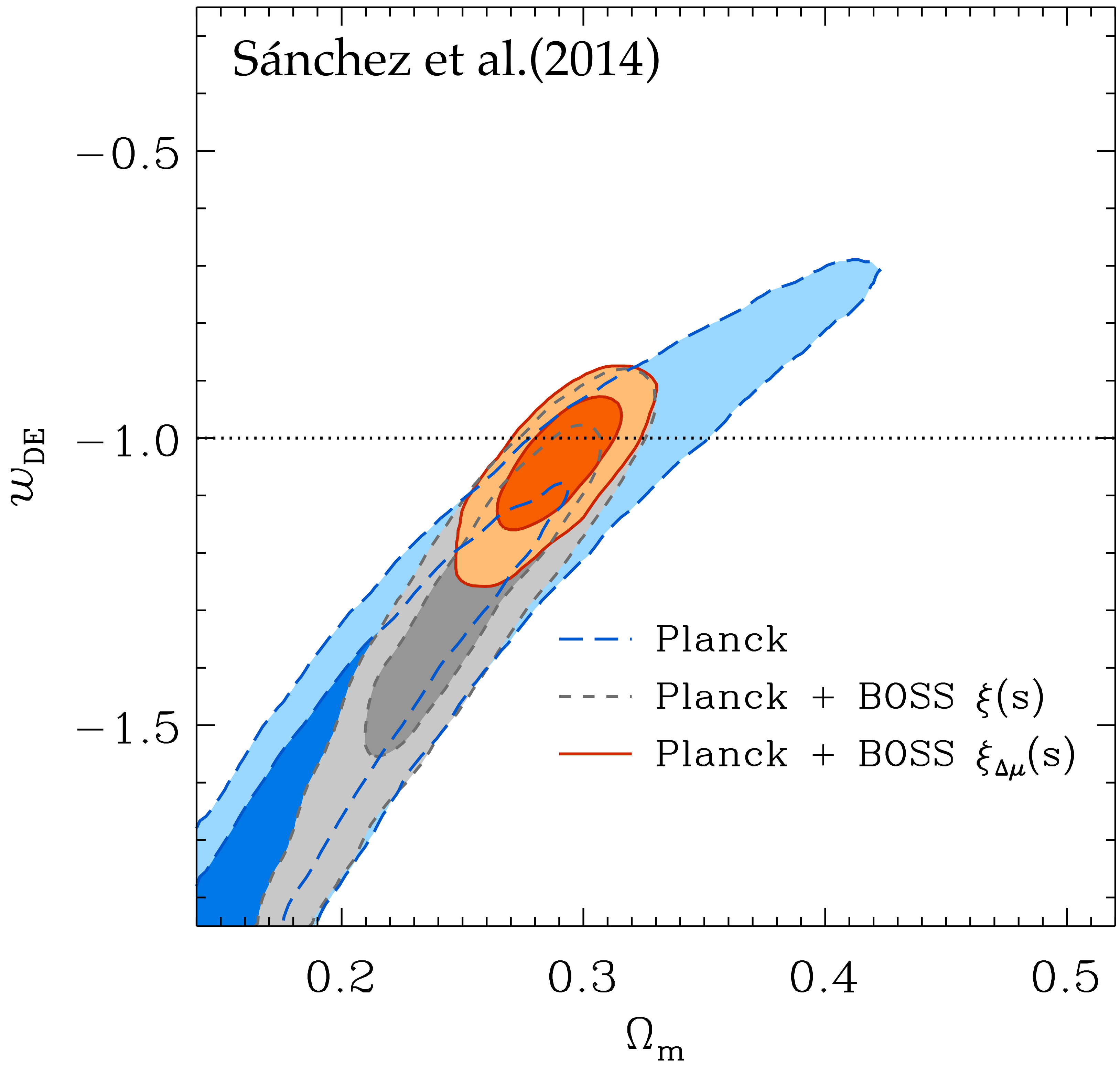

Planck + BOSS $\xi(s)$

$$\Omega_{\mathrm{m}} = 0.249^{+0.034}_{-0.026}$$

$$w_{\mathrm{DE}} = -1.31^{+0.21}_{-0.16}$$

Planck + BOSS $\xi_{\Delta\mu}(s)$

$$\Omega_{\mathrm{m}} = 0.288 \pm 0.016$$

$$w_{\mathrm{DE}} = -1.051 \pm 0.076$$

Anisotropic clustering

- BOSS DR12 clustering wedges:

Sánchez et al. (2016a)

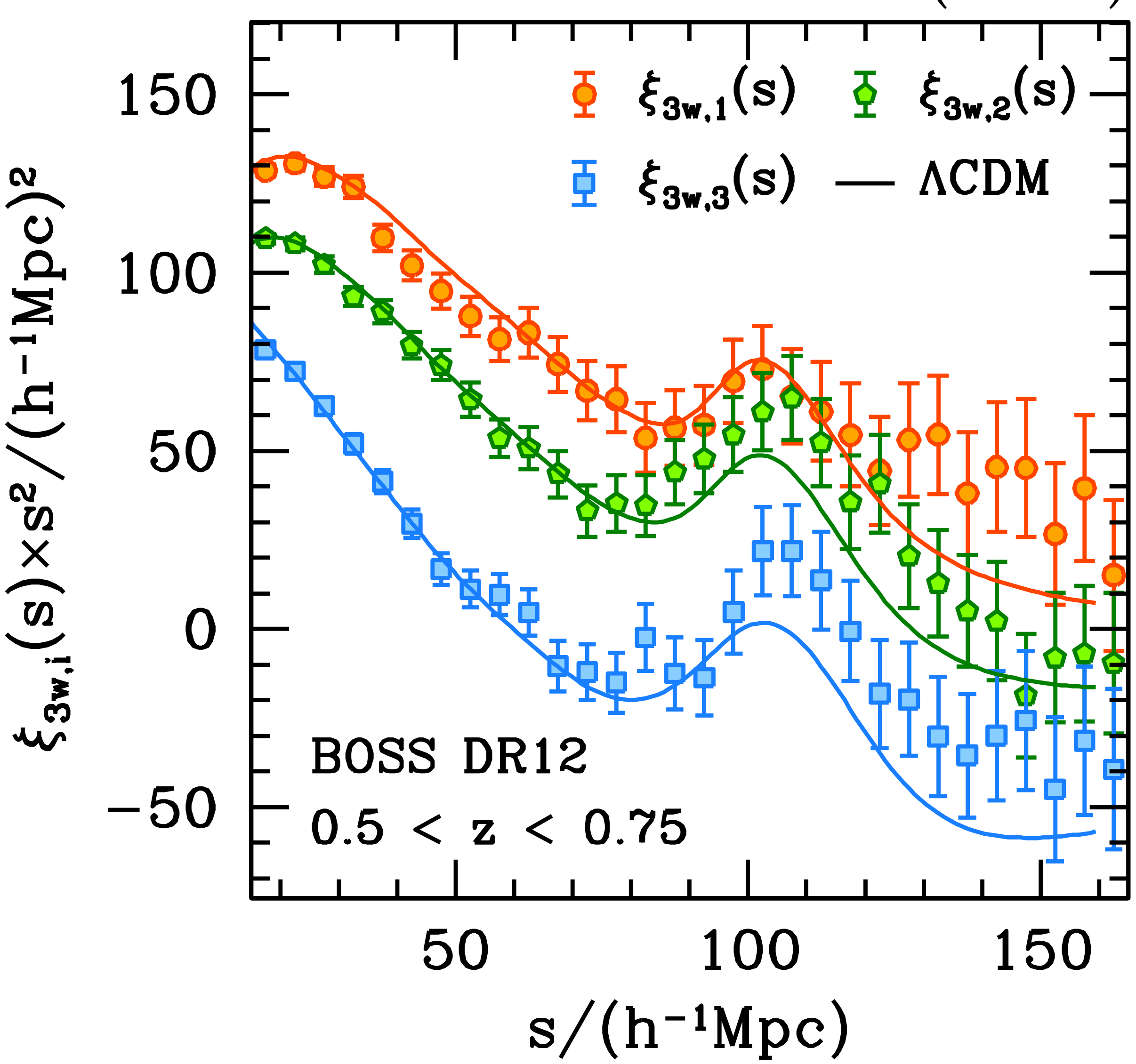

Grieb et al. (2016)

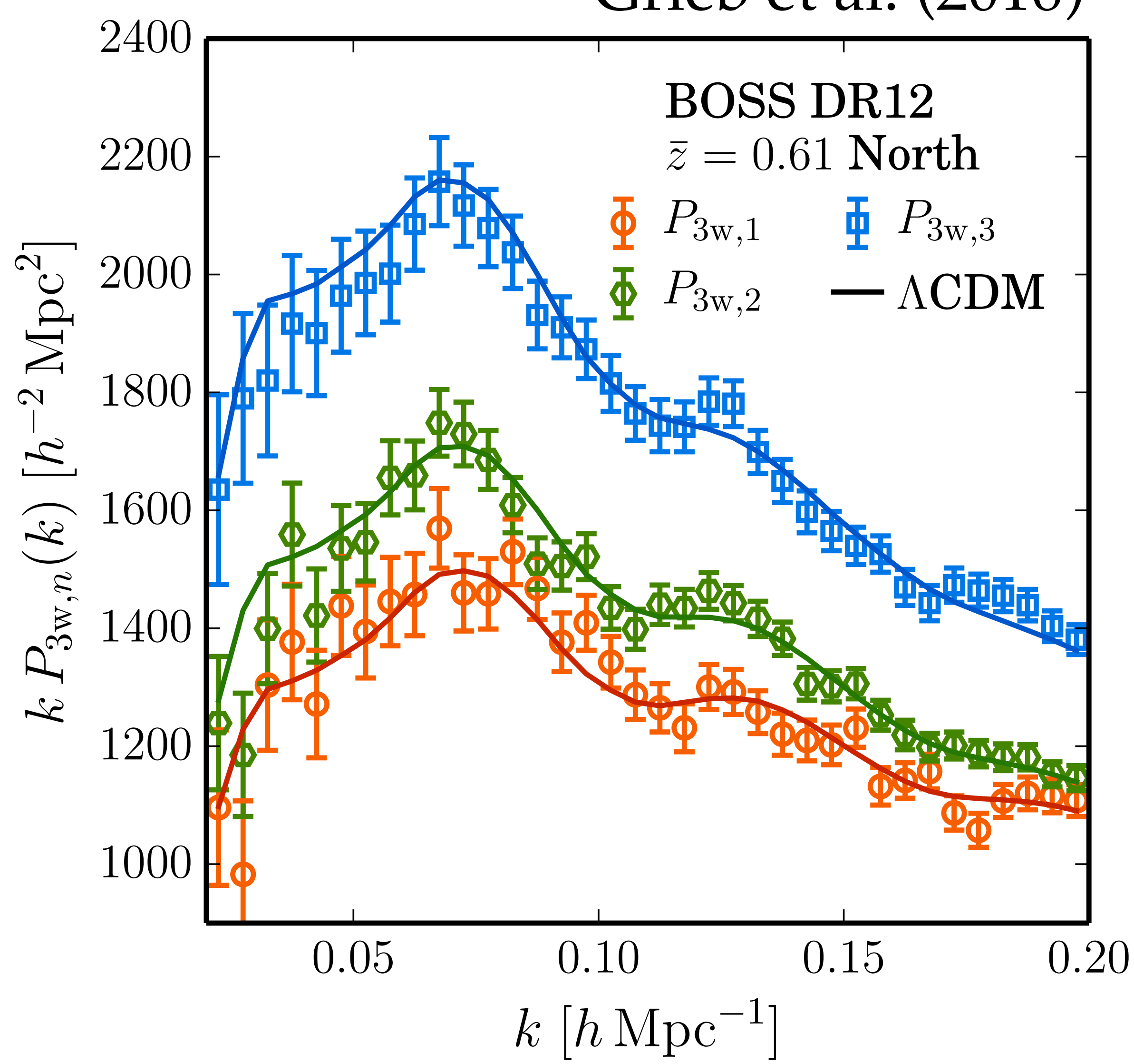

The dark energy equation of state

- Our results are consistent with the ΛCDM model.
- Assuming a constant w_{DE}

$$\boxed{\begin{aligned} w_{\mathrm{DE}} &= -0.991 \pm 0.055 \\ \Omega_{\mathrm{m}} &= 0.308 \pm 0.013 \end{aligned}}$$

Sánchez et al. (2017a)

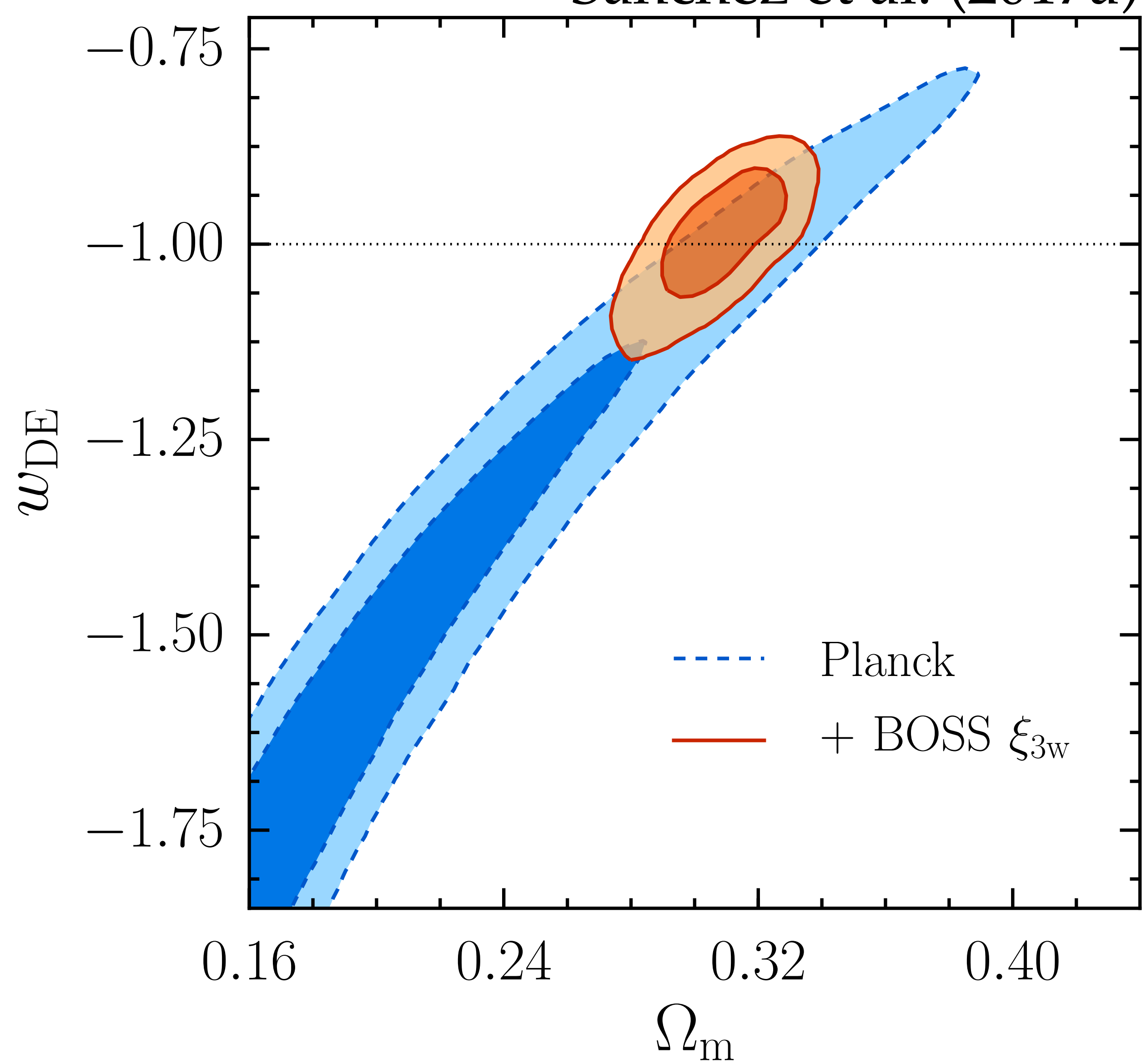

The dark energy equation of state

- Our results are consistent with the ΛCDM model.
- Assuming a constant w_{DE}

$$\boxed{\begin{aligned} w_{\mathrm{DE}} &= -0.991 \pm 0.055 \\ \Omega_{\mathrm{m}} &= 0.308 \pm 0.013 \end{aligned}}$$

- Adding SN information

$$\boxed{\begin{aligned} w_{\mathrm{DE}} &= -0.996 \pm 0.042 \\ \Omega_{\mathrm{m}} &= 0.306 \pm 0.010 \end{aligned}}$$

Sánchez et al. (2017a)

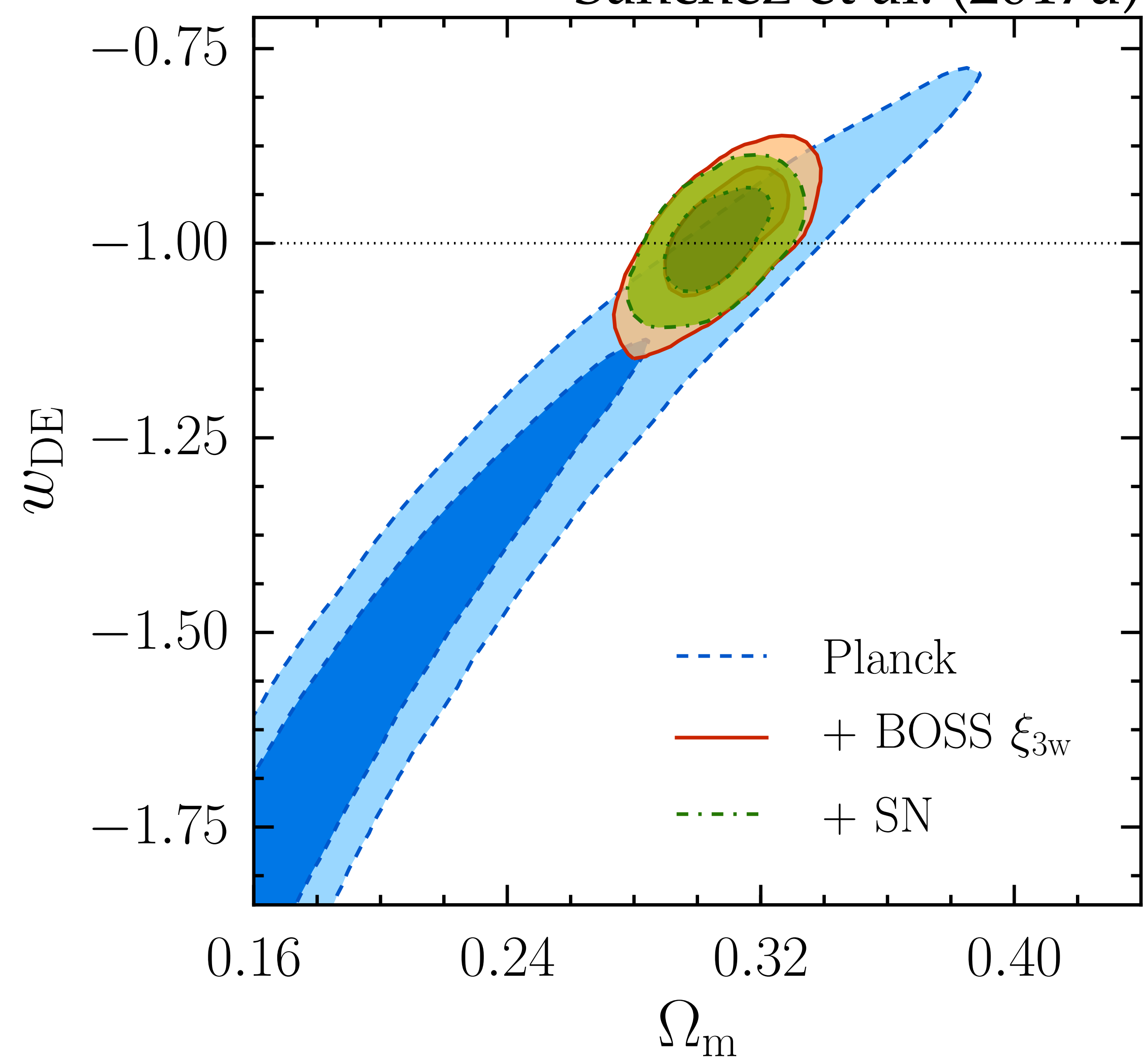

The dark energy equation of state

- Our results are consistent with the ΛCDM model.
- Allowing w_{DE} to evolve as

$$w_{\mathrm{DE}}(a) = w_0 + w_a\,(1 - a)$$

$$\boxed{\begin{aligned} w_0 &= -0.92 \pm 0.11 \\ w_a &= -0.32 \pm 0.40 \end{aligned}}$$

Sánchez et al. (2017a)

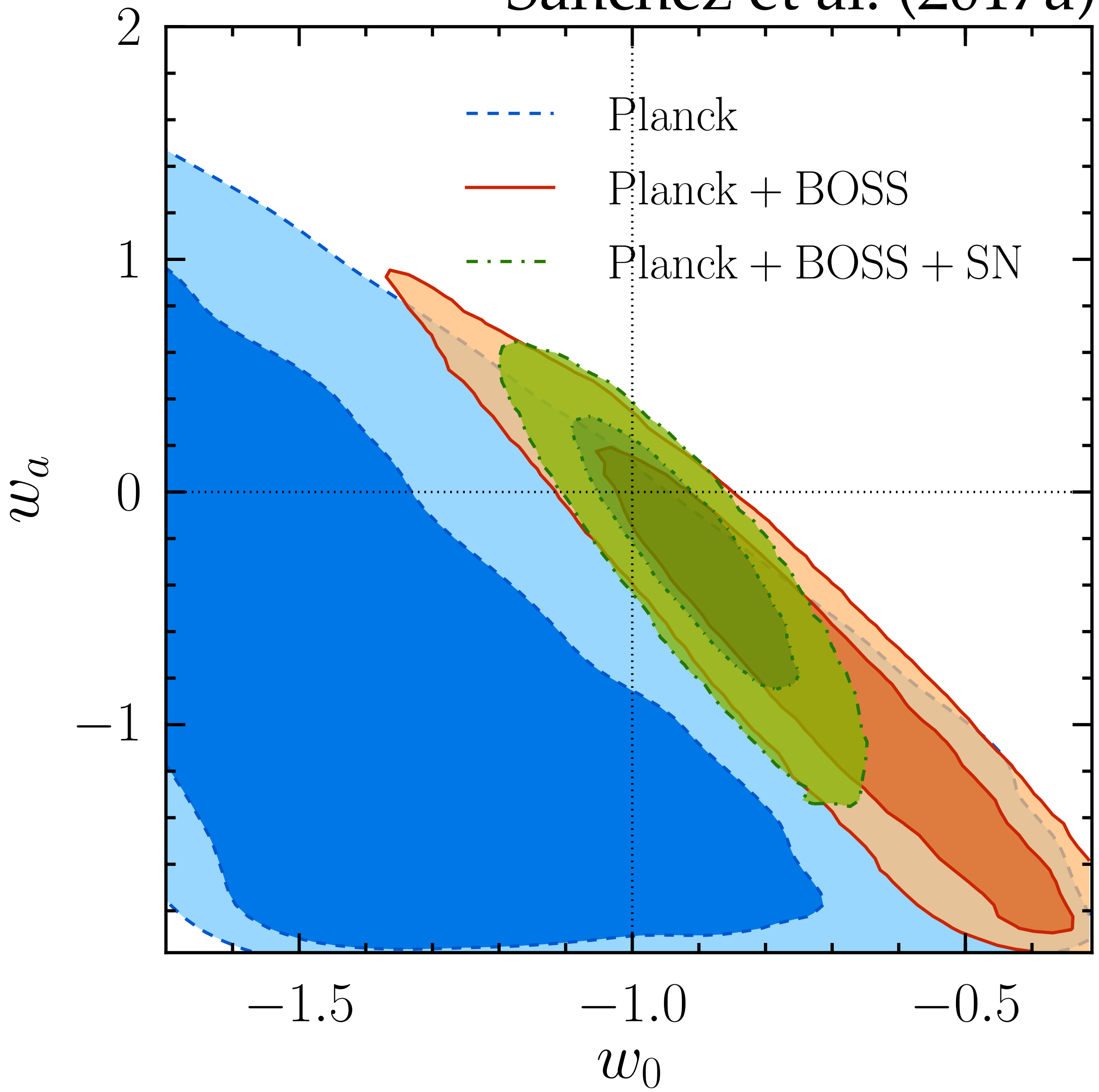

Testing general relativity

- General relativity predicts

$$f(z) = \Omega_{\rm m}(z)^{\gamma}$$

with $\gamma \simeq 0.55$

- Deviations from this value could indicate a failure of GR.

- Combining Planck+BOSS

$$\gamma = 0.61 \pm 0.08$$

Sánchez et al. (2017a)

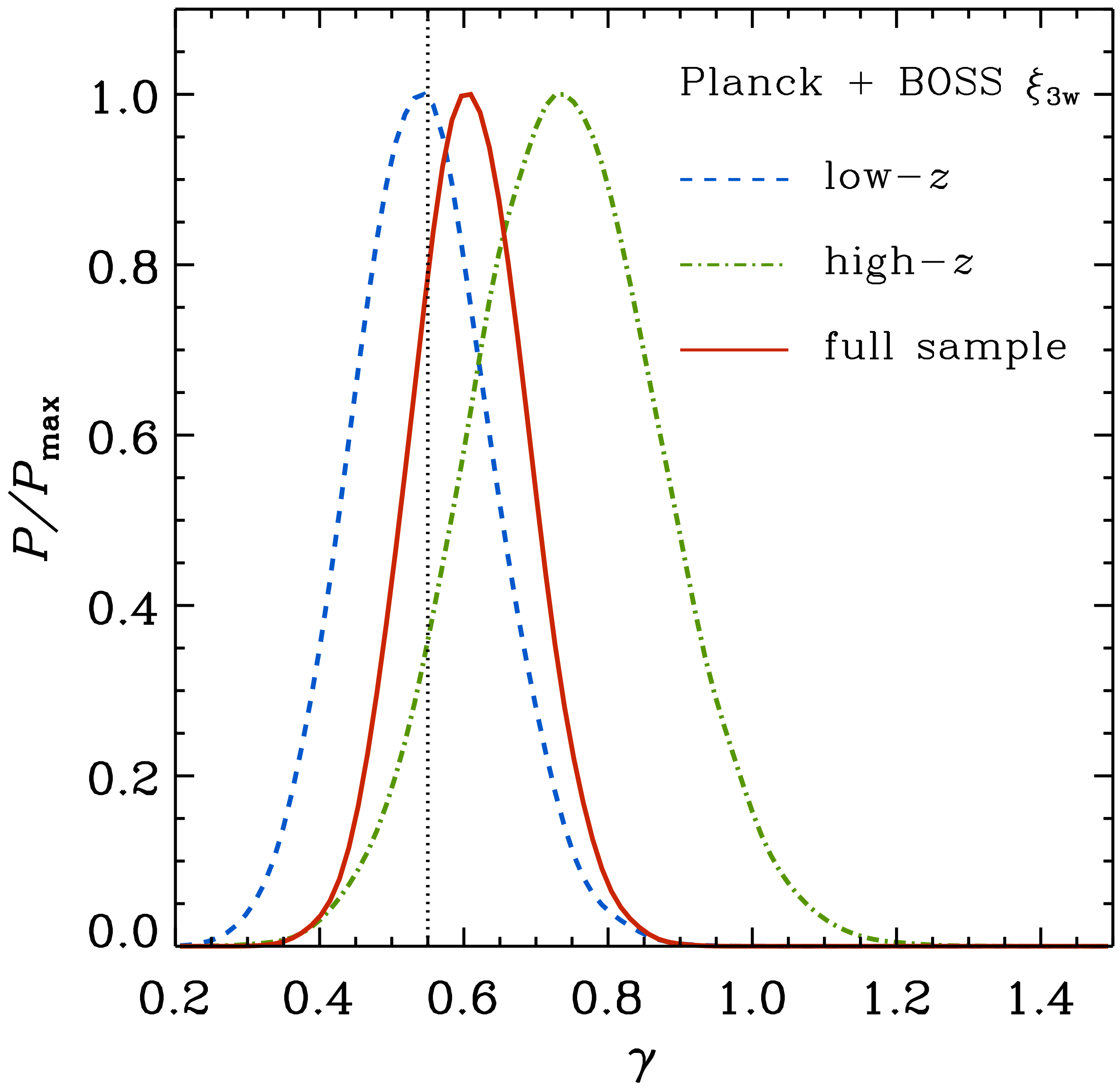

BOSS consensus constraints

- Galaxy surveys require considerable resources from the community.
- Effort to maximise the information extracted from these data sets.
- Question often posed as which statistic or method should be used (e.g. $P(k)$ vs $\xi(s)$).
- Additional information can be obtained from the combination of different results.

BOSS consensus constraints

- Galaxy clustering information can be compressed into a set of parameters $\mathbf{D}$ (e.g. $D_{\mathrm{M}}(z)/r_{\mathrm{d}}, H(z)r_{\mathrm{d}}, f\sigma_8(z)$)

- A set of m measurements $\mathbf{D}_i$, $\mathbf{C}_{ii}$ can be combined into a set of *consensus constraints* $\mathbf{D}_{\mathrm{c}}$, $\mathbf{C}_{\mathrm{c}}$ (Sánchez et al. 2017b)

$$\left.\begin{array}{l} \mathbf{D}_{\mathrm{tot}} = (\mathbf{D}_1, \cdots, \mathbf{D}_m) \\ \\ \mathbf{C}_{\mathrm{tot}} = \begin{pmatrix} \mathbf{C}_{11} & \cdots & \mathbf{C}_{1m} \\ \vdots & \ddots & \vdots \\ \mathbf{C}_{m1} & \cdots & \mathbf{C}_{mm} \end{pmatrix} \end{array}\right\} \mathbf{D}_{\mathrm{c}},\ \mathbf{C}_{\mathrm{c}}$$

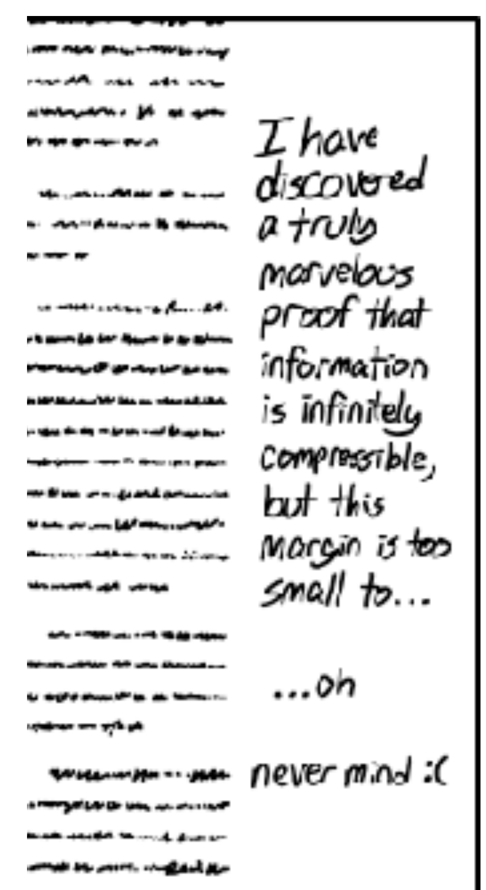

http://xkcd.com/

BOSS consensus constraints

- Application to BOSS DR12 results:

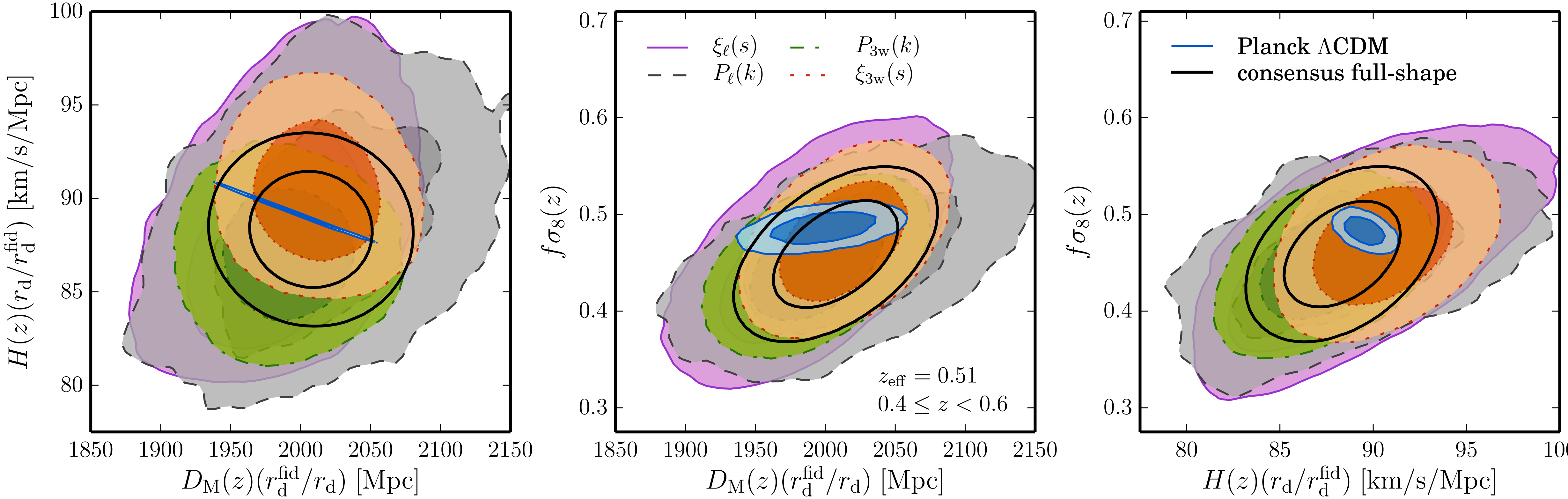

Alam et al. (2017)

- Consensus constraints are up to 20% tighter than the most accurate measurement from the original set.

- Good agreement with the Planck ΛCDM prediction.

BOSS consensus constraints

- Application to BOSS DR12 results:

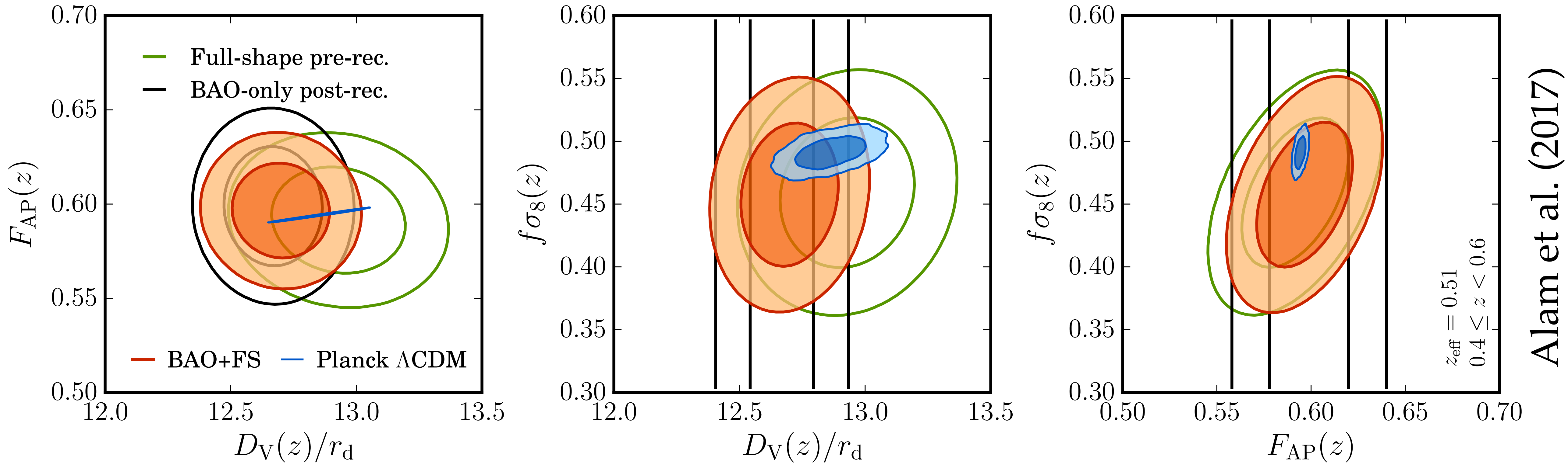

- BAO-only and full-shape fits are combined into our final consensus constraints:

https://www.sdss3.org/science/boss_publications.php

BOSS consensus constraints

- Consensus constraints on $D_{\mathrm{M}}(z)/r_{\mathrm{d}}, H(z)r_{\mathrm{d}}, f\sigma_8(z)$ are in agreement with Planck ΛCDM predictions.
- The error bars include statistical and systematic errors.

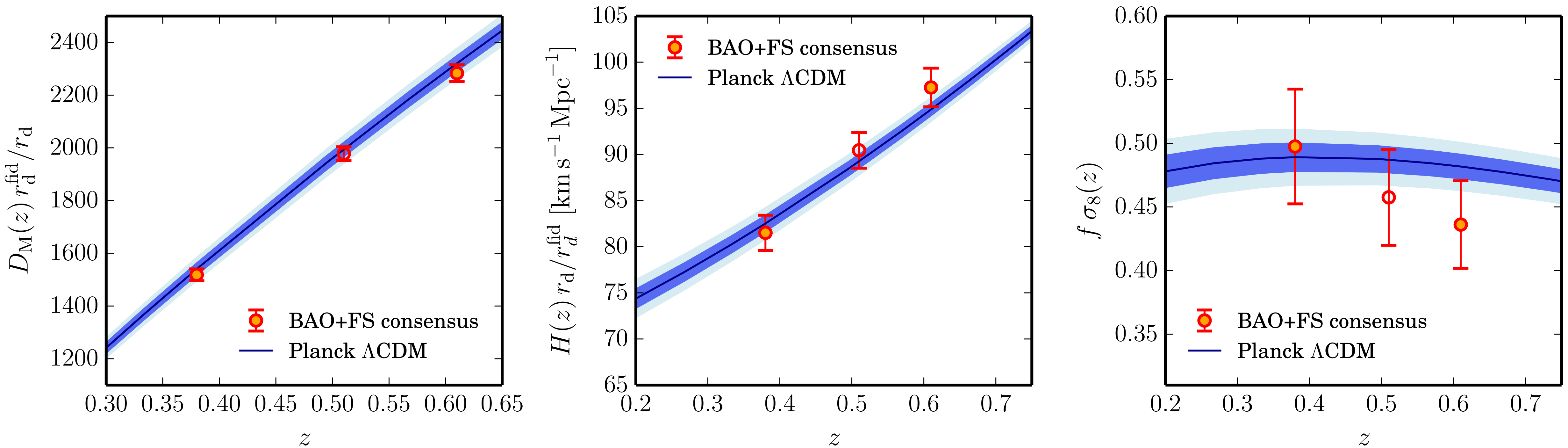

- Cosmological implications explored in Alam et al. (2017)

Future galaxy surveys

- A new generation of large volume galaxy surveys:
  - **eBOSS**: LRGs, ELGs, QSO at $0.7 < z < 2.8$
  - **HETDEX**: Ly-α emitters, $1.9 < z < 3.5$
  - **PFS**: ELGs, $0.6 < z < 2.4$
  - DESI: LRGs, ELGs, QSO at $0.4 < z < 3.5$
  - **Euclid**: H-α emitters, $0.6 < z < 2$

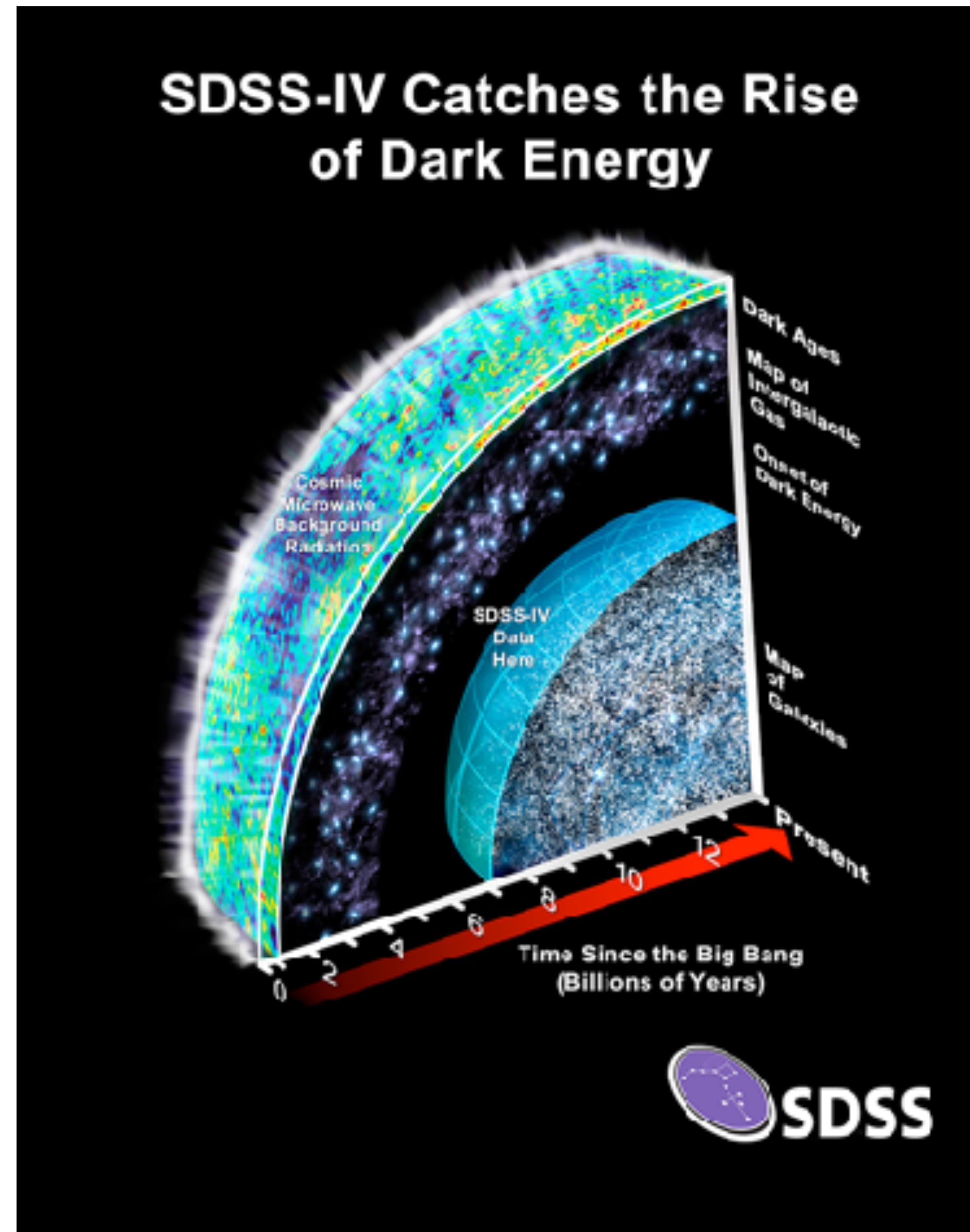

BAO & RSD forecasts

- The Fisher information matrix is defined as

$$F_{ij} = -\left\langle \frac{\partial^2 \ln \mathcal{L}}{\partial\theta_i \partial\theta_j} \right\rangle\bigg|_{\boldsymbol{\theta}_0}$$

$$\ln \mathcal{L}(\boldsymbol{\theta}) = \ln \mathcal{L}(\boldsymbol{\theta}_0) - \frac{1}{2}\left(\boldsymbol{\theta} - \boldsymbol{\theta}_0\right)^T \mathbf{F}\left(\boldsymbol{\theta} - \boldsymbol{\theta}_0\right)$$

$$\Rightarrow C(\theta_i, \theta_j) \simeq F_{ij}^{-1}$$

- Use a model to predict $\xi_\ell(s)$, $\xi_{\rm w}(s)$, $P_\ell(k)$, $P_{\rm w}(s)$.

- Assume Gaussian covariance matrices (Grieb et al. 2016)

Future galaxy surveys

- State of the art of galaxy clustering measurements…

Sánchez et al. (2016a)

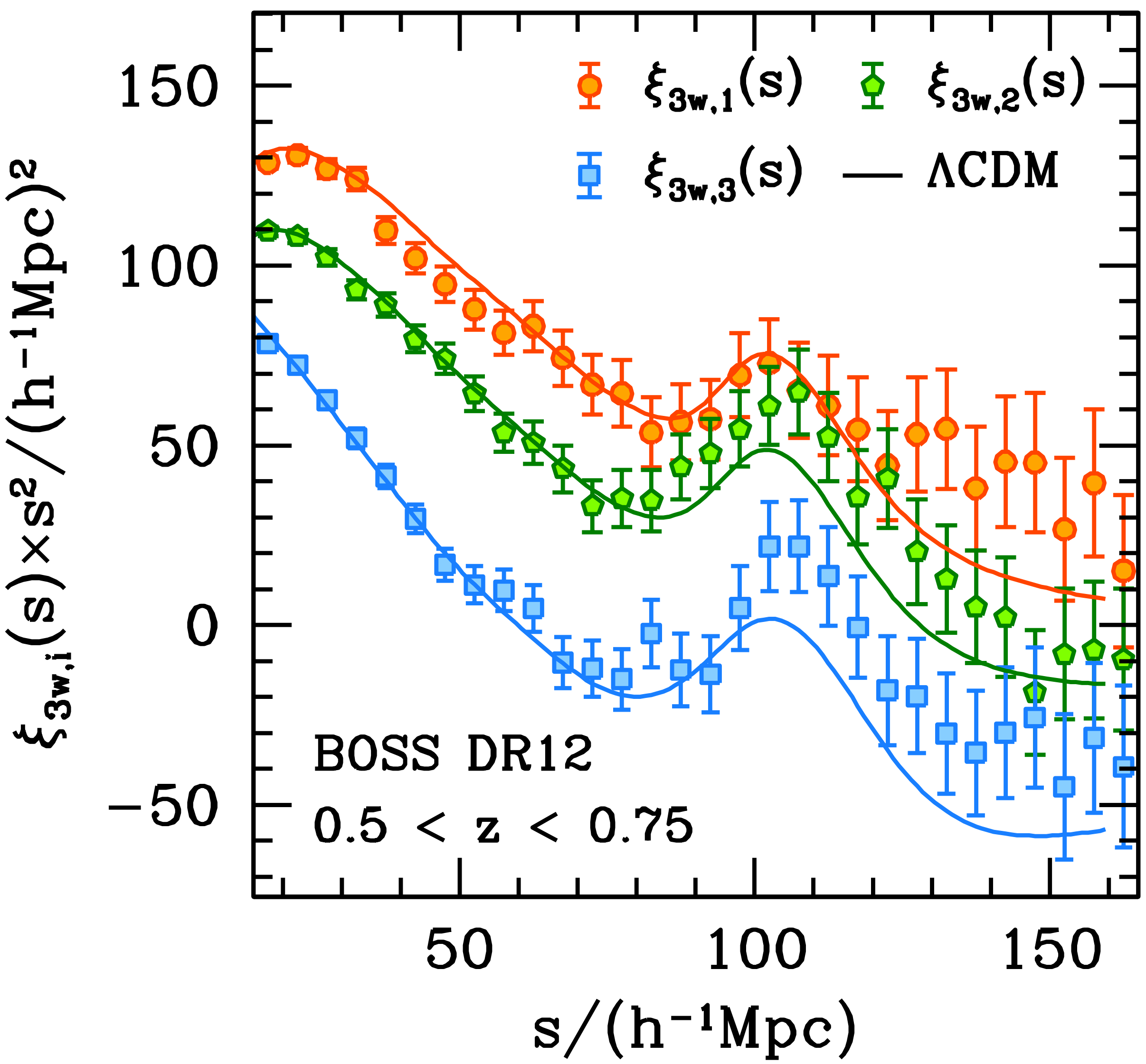

Grieb et al. (2016)

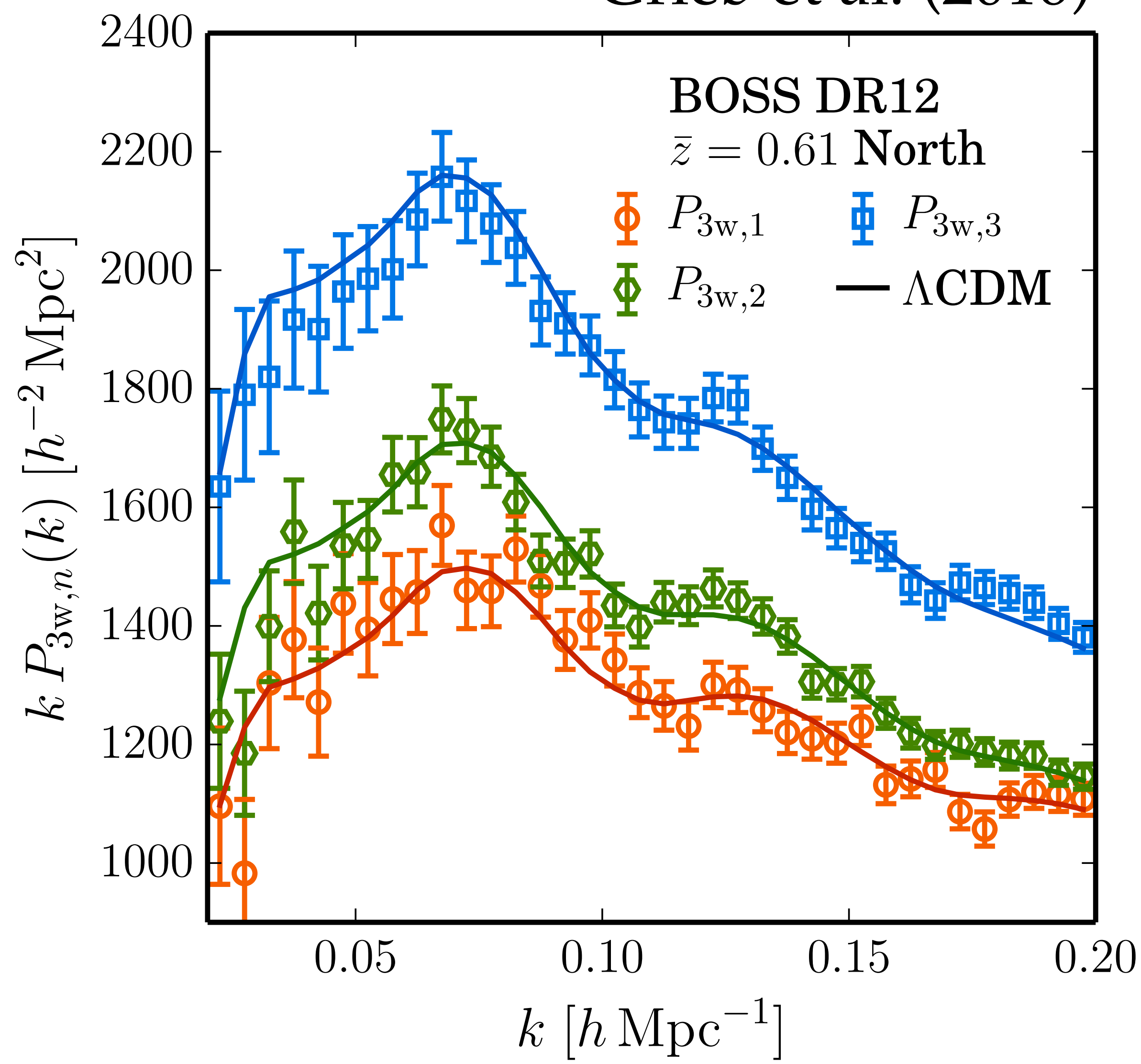

Future galaxy surveys

- Predictions for Euclid clustering measurements.

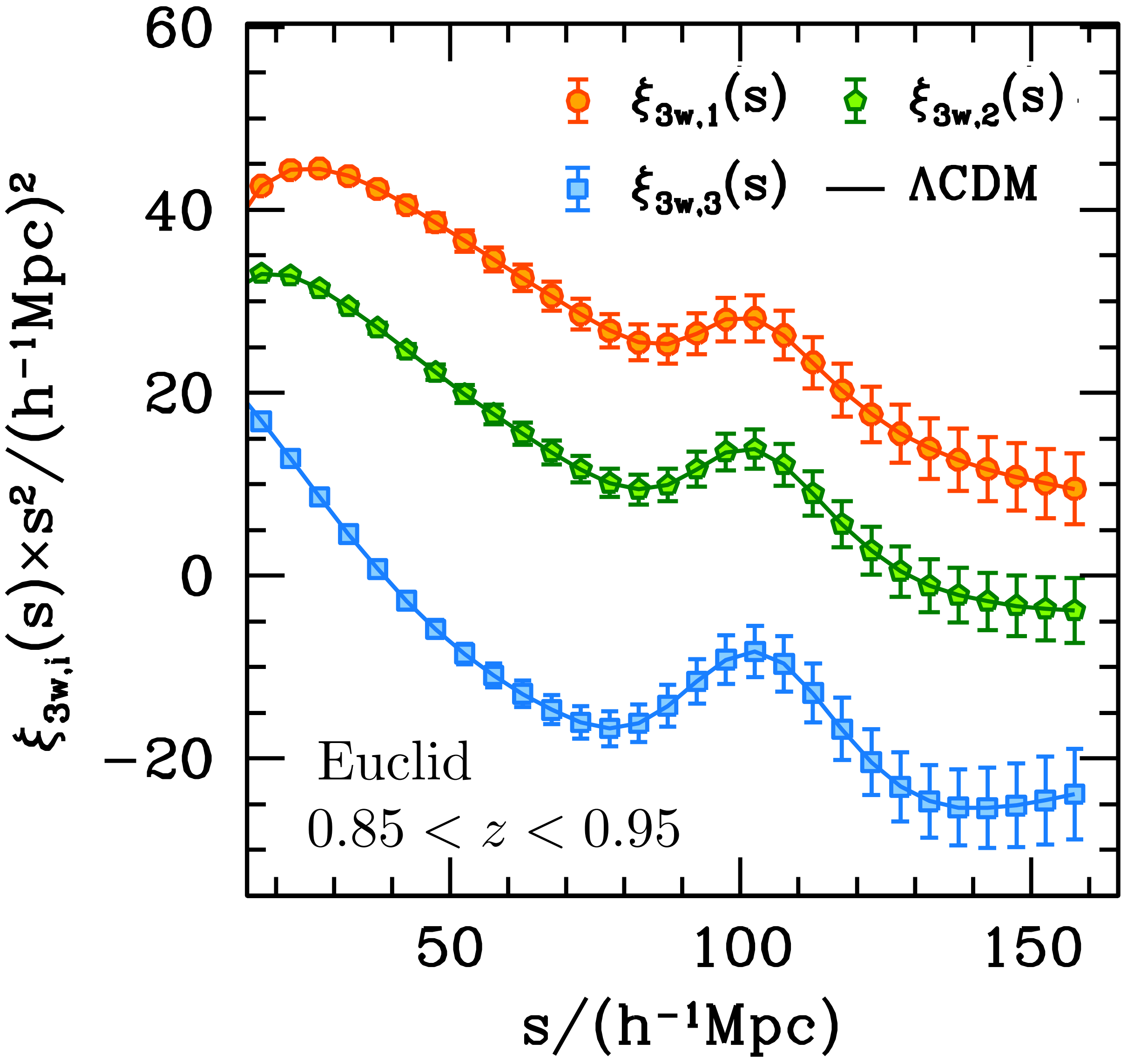

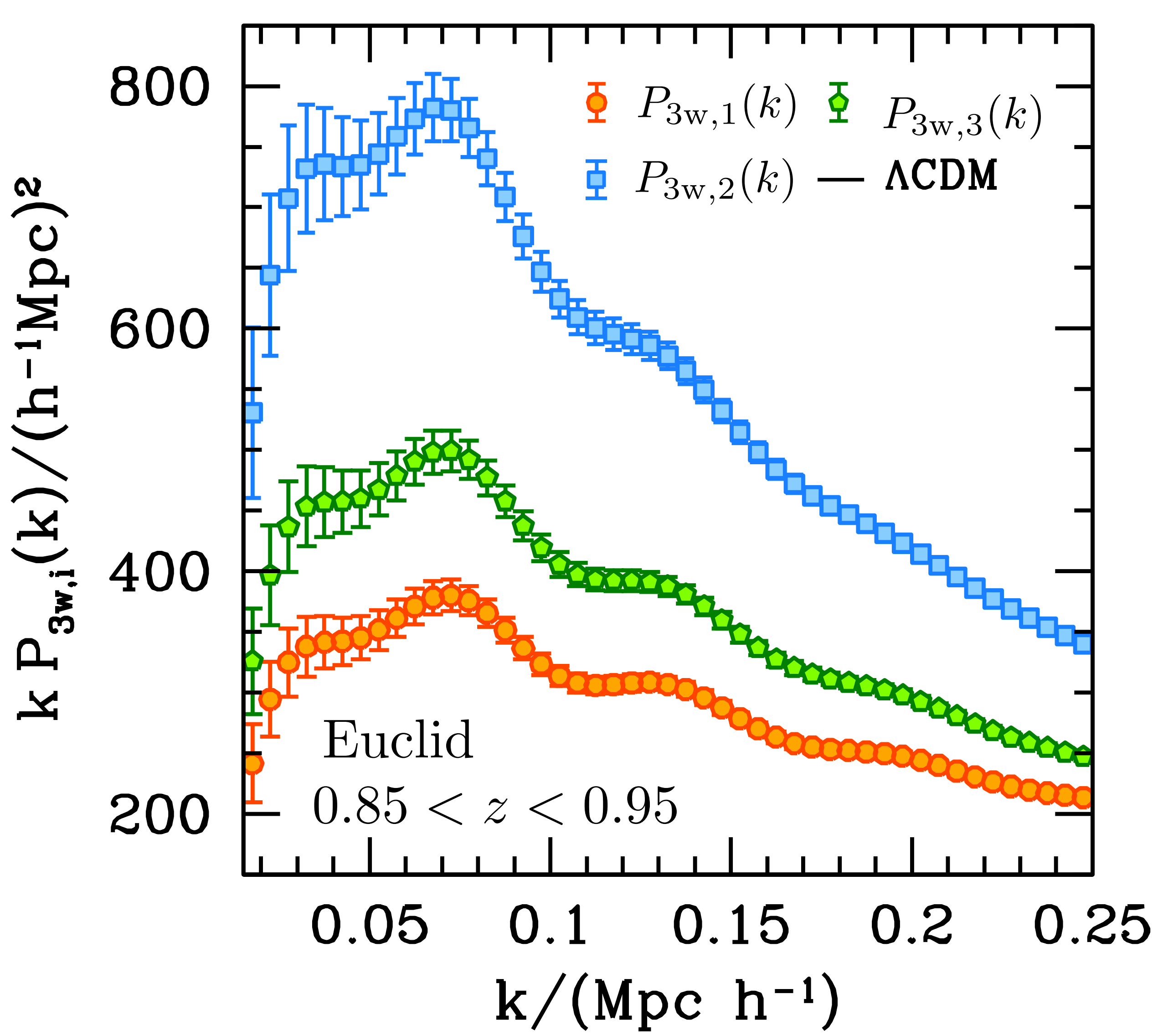

Eucid GC forecasts

- Construct the likelihood function $\mathcal{L} \propto \mathrm{e}^{-\chi^2/2}$, where

$$\chi^2 = (\mathbf{D} - \mathbf{T})^t \mathbf{C}^{-1} (\mathbf{D} - \mathbf{T})$$

- The fisher information matrix is simply given by

$$F_{ij} = \frac{1}{2} \frac{\partial^2 \chi^2}{\partial \theta_i \partial \theta_j}$$

- BOSS forecasts are in good agreement with real results.

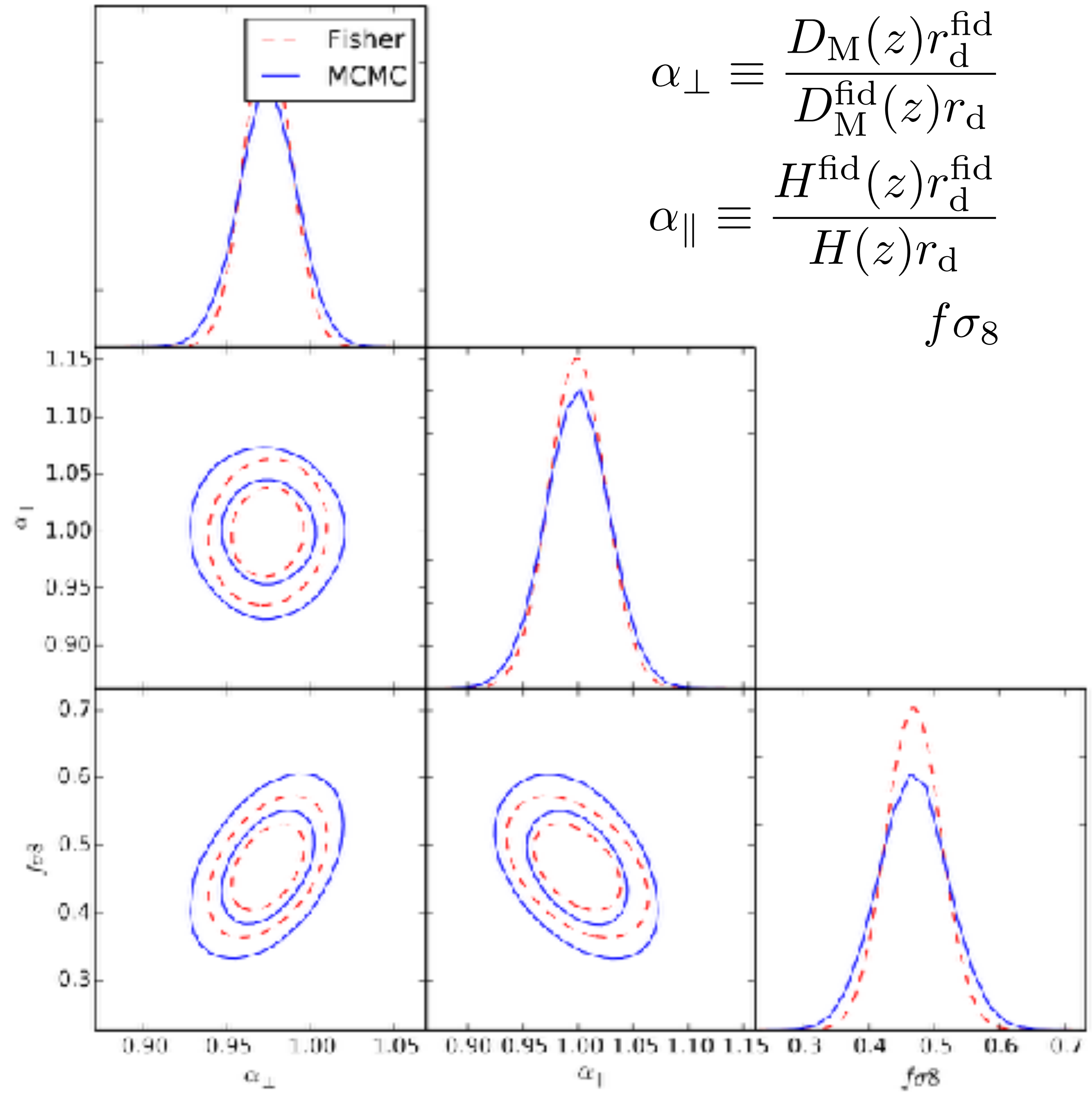

$$\alpha_\perp \equiv \frac{D_\mathrm{M}(z) r_\mathrm{d}^\mathrm{fid}}{D_\mathrm{M}^\mathrm{fid}(z) r_\mathrm{d}}$$

$$\alpha_\parallel \equiv \frac{H^\mathrm{fid}(z) r_\mathrm{d}^\mathrm{fid}}{H(z) r_\mathrm{d}}$$

$$f\sigma_8$$

Future galaxy surveys

- A new generation of large volume galaxy surveys:
  - **eBOSS**: LRGs, ELGs, QSO at $0.7 < z < 2.8$
  - **HETDEX**: Ly-α emitters, $1.9 < z < 3.5$
  - **PFS**: ELGs, $0.6 < z < 2.4$
  - DESI: LRGs, ELGs, QSO at $0.4 < z < 3.5$
  - **Euclid**: H-α emitters, $0.6 < z < 2$

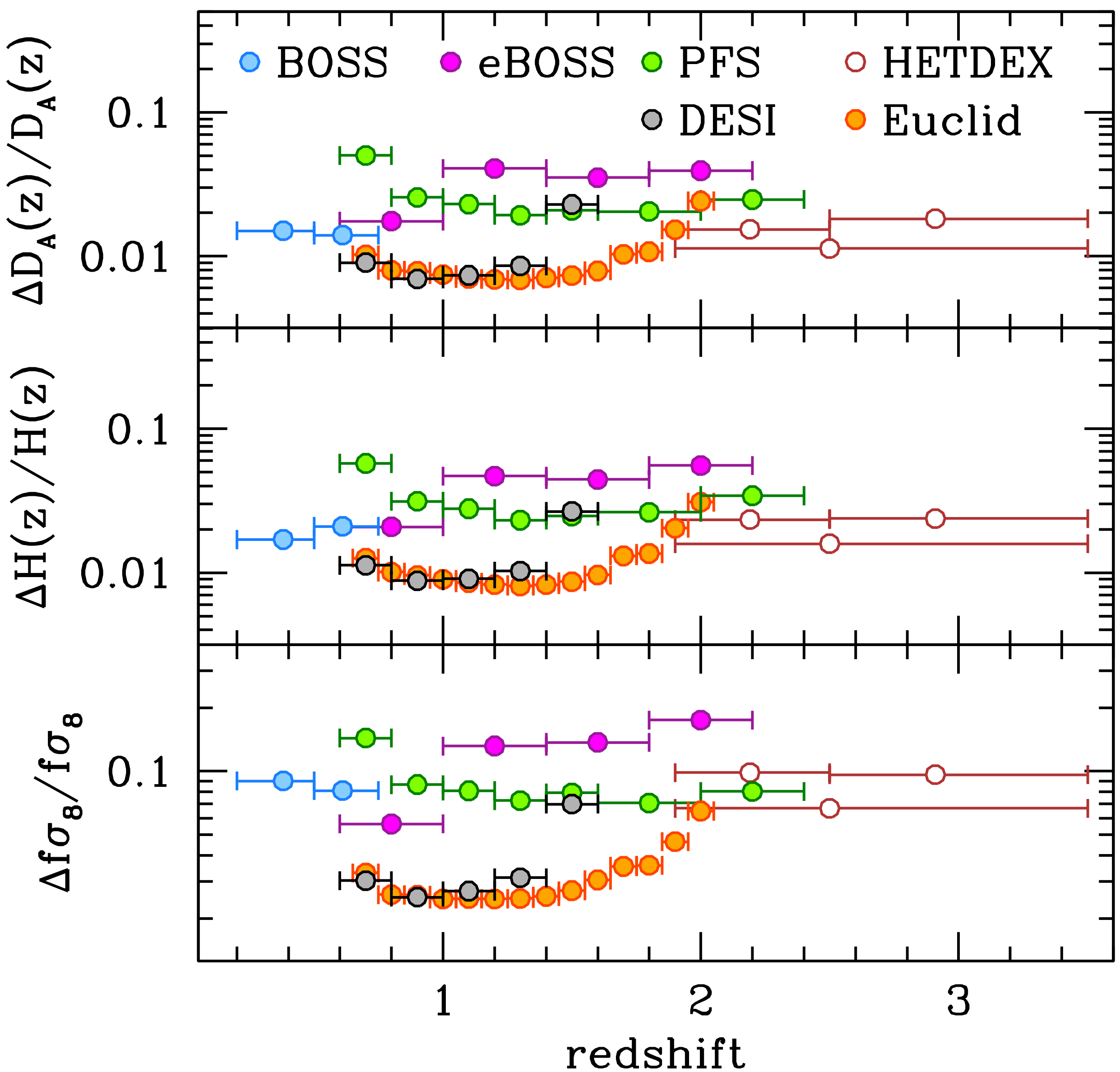

Lecture 2: RSD

- Redshift-space distortions (RSD).
- The density - velocity relation.
- Impact of RSD on clustering measurements.
- Modelling of RSD beyond the linear regime.
- Current cosmological constraints from BAO & RSD.
- Forecasts for future surveys.